Stereodynamics of 6-*exo*-Phenylcyclohexadienyl Complexes of Manganese and Rhenium

R. D. Pike, T. J. Alavosus, W. H. Hallows, N. S. Lennhoff, W. J. Ryan, and D. A. Sweigart*

Department of Chemistry, Brown University, Providence, Rhode Island 02912

C. H. Bushweller,* C. M. DiMeglio, and J. H. Brown

Department of Chemistry, University of Vermont, Burlington, Vermont 05405

Received November 6, 1991

The series of neutral and cationic complexes $[(PhC_6H_6)Mn(CO)_2NO]PF_6$, $[(PhC_6H_6)Mn(PMe_3)_2NO]PF_6$, $(PhC_6H_6)Mn(CO)_2PMe_3$, $(PhC_6H_6)Mn(PMe_3)_2CO$, $[(PhC_6HMe_5)Mn(CO)_2NO]PF_6$, and $[(PhC_6HMe_5)Re(CO)_2NO]PF_6$ all show a decoalescence of the ^1H NMR spectrum below room temperature, allowing identification of preferred equilibrium conformations and measurement of barriers to conformational exchange. For these six systems, there is an essentially exclusive preference for the C_1-symmetric enantiomeric conformers that have the unique unidentate ligand eclipsing C2 or C4 of the cyclohexadienyl ring. The barriers (ΔG^*) to conformational exchange vary in a range from 9.2 to 11.4 kcal mol^{-1}. Substitution of rhenium for manganese has no effect on conformational preference or on the barrier to conformational exchange. For the complexes $[(PhC_6H_6)Mn(NO)dppen]PF_6$, $[(PhC_6H_6)Mn(NO)dppe]PF_6$, $(PhC_6H_6)Mn(CO)dppe$, and $[(PhC_6H_6)Mn(NO)arphos]PF_6$, which have a bidentate ligand, variable-temperature ^1H and $^{31}P\{^1H\}$ NMR spectra reveal differences in conformational preference. In the dppen/NO derivative, there is an exclusive preference for the C_1-symmetric enantiomers in which a phosphorus atom eclipses C6 of the cyclohexadienyl ring and NO eclipses C2 or C4 of the cyclohexadienyl ring. In the dppe/NO complex, the C_1 forms dominate (98%) but there is a detectable concentration of the C_s conformer in which NO eclipses C6 of the cyclohexadienyl ring. In the dppe/CO complex, there is an essentially statistical distribution of conformational populations among the C_1 and C_s forms. In the last two complexes, the barrier for a C_1 to C_1 conversion is higher than that for the C_1 to C_s process. The chiral arphos/NO system shows a strong preference for the conformer that has phosphorus eclipsing C6 of the cyclohexadienyl ring (88% at 231 K) and a small concentration of the form that has arsenic eclipsing C6 (12%). The barriers for conformational exchange in these bidentate analogues vary from 10.0 to 12.9 kcal/mol. The assignment of certain NMR signals for the complexes which have a bidentate ligand was aided by an X-ray structural study of $[(6\text{-}exo\text{-}PhC_6H_6)Mn(NO)dppe]PF_6$, which crystallizes in the monoclinic space group $P2_1/c$ with $a = 11.665$ (2) Å, $b = 16.961$ (6) Å, $c = 18.182$ (4) Å, $\beta = 95.58$ (2)°, $Z = 4$, $R = 0.039$, and $R_w = 0.044$. In the crystal, the dppe/NO complex cation exists as two C_1-symmetric enantiomeric conformations; in each conformation, a phosphorus atom eclipses C6 of the cyclohexadienyl ring. These conformations are the same as the dominant conformations observed in solution.

Introduction

A variety of intramolecular conformational exchange processes occur in organometallic complexes.[1,2] One common process is π-ligand rotation, occurring about an axis normal to the π-system and located at its center. This phenomenon has been studied for a wide variety of unsaturated hydrocarbon ligands, ranging from η^2-alkenes and -alkynes to η^7-trienyls. The free energy of activation (ΔG^*) for π-polyene rotation is not due to changes in hapticity during rotation, but rather, it is dependent upon molecular orbital overlap that selectively stabilizes the equilibrium conformations.[3] Rotation barriers (ΔG^*) between 7 and 20 kcal mol^{-1} for a variety of polyene systems have been measured by complete theoretical lineshape simulation of dynamic NMR (DNMR) spectra.[1]

Although rotation of the acyclic pentadienyl ligand in a variety of metal complexes has been studied,[3-5] there have been few studies of rotation of the symmetrically equivalent cyclohexadienyl ring.[6-8] Steric and orbital considerations indicate that cyclohexadienylmetal tripod species will adopt conformation 1 rather than 2 or a

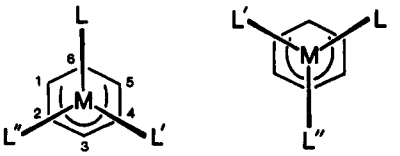

1 2

staggered conformation (projections 1 and 2 are viewed along the rotational axis).[4] Restricted cyclohexadienyl ring rotation leads to decoalescence of the low-temperature $^{13}C\{^1H\}$ NMR spectra of a series of substituted $[(cyclohexadienyl)Fe(CO)_3]^+$ complexes.[7] In these systems, a methyl or methoxy substituent at the C3 position lowers the barrier to rotation, while substitution at the C2 position increases the barrier.[7] $^{31}P\{^1H\}$ DNMR spectroscopy has been used to study cyclohexadienyl ring rotation in $[(C_6H_7)M(CO)_2eptb]^{0,+}$ and $[(C_6H_7)M(CO)(eptb)_2]^{0,+}$ (M = Mn, Fe^+, Ru^+; eptb = 4-ethyl-1-phospha-2,6,7-trioxabicyclo[2.2.2]octane).[8] The rotation barriers (ΔG^*) are in the range 10–11 kcal mol^{-1} for manganese and iron and 12–13 kcal mol^{-1} for ruthenium.

We have been interested in the reaction and structural chemistry of cyclohexadienylmanganese and -rhenium complexes for a number of years.[9-13] During the course

(1) Mann, B. E. In *Comprehensive Organometallic Chemistry*; Pergamon Press: Oxford, U.K., 1986; Vol. 3, Chapter 20.
(2) Faller, J. W. *Adv. Organomet. Chem.* **1977**, *16*, 211.
(3) Albright, T. A.; Hofmann, P.; Hoffmann, R. *J. Am. Chem. Soc.* **1977**, *99*, 7546. Hoffmann, R.; Albright, T. A.; Thorn, D. L. *Pure Appl. Chem.* **1978**, *50*, 1.
(4) Hoffmann, R.; Hofmann, P. *J. Am. Chem. Soc.* **1976**, *98*, 598.
(5) Dobosh, P. A.; Gresham, D. G.; Kowalski, D. J.; Lillya, C. P.; Magyar, E. S. *Inorg. Chem.* **1978**, *17*, 1775. Ernst, R. D. *Chem. Rev.* **1988**, *88*, 1255. Bleeke, J. R.; Hays, M. K.; Wittenbrink, R. J. *Organometallics* **1988**, *7*, 1417. Bleeke, J. R.; Rauscher, D. J. *Organometallics* **1988**, *7*, 2328.
(6) Helling, J. F.; Braitsch, D. M. *J. Am. Chem. Soc.* **1970**, *92*, 7209.
(7) Harland, L.; Stephenson, G. R.; Whittaker, M. J. *J. Organomet. Chem.* **1984**, *263*, C30.
(8) Whitesides, T. H.; Budnik, R. A. *Inorg. Chem.* **1975**, *14*, 664.

0276-7333/92/2311-2841$03.00/0

of these investigations, we obtained DNMR evidence for polyene ring rotation in a variety of 6-*exo*-phenylcyclohexadienyl complexes. This paper reports the results of ^1H and $^{31}P\{^1H\}$ DNMR studies of cyclohexadienyl ring rotation in a series of complexes (**3**; M = Mn, Re; X = H, Me). The ligand set (L, L′, L″) includes CO, NO, PMe_3,

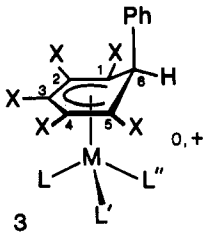

3

dppe (1,2-bis(diphenylphosphino)ethane), dppen (*cis*-1,2-bis(diphenylphosphino)ethene), and arphos (1-(diphenylphosphino)-2-(diphenylarsino)ethane). The slow-exchange DNMR spectrum of each complex allowed identification of the preferred equilibrium conformations. Theoretical simulations of the exchange-broadened DNMR spectra allowed measurement of the barriers to cyclohexadienyl ring rotation. In the dppe, dppen, and arphos complexes, theoretical simulations of the DNMR spectra show that stereomutation of the metallacyclic ring and cyclohexadienyl ring rotation occur in concert.

Experimental Section

The complexes were prepared as previously described,[9,12-15] with the exception of the new compounds listed below. All cationic complexes were purified by growing crystals via slow diethyl ether diffusion into a filtered dichloromethane solution of the complex.

[(PhC$_6$H$_6$)Mn(NO)arphos]PF$_6$. [(PhC$_6$H$_6$)Mn(CO)$_2$NO]PF$_6$ (238 mg, 0.542 mmol) and arphos (243 mg, 0.550 mmol, Pressure Chemical Co.) were suspended in 50 mL of CH_2Cl_2, and the suspension was refluxed. The color quickly changed from yellow to orange as the expected product of nucleophilic addition to the ring formed, (6-*exo*-Ph-5-*exo*-arphos-η^4-cyclohexa-1,3-diene)Mn(CO)$_2$NO$^+$ (ν_{CO}, ν_{NO} = 2053, 2002, 1764 cm^{-1}).[9] As the solution slowly became reddish, the monocarbonyl replacement (2031, 1787 cm^{-1}) and finally the dicarbonyl replacement (1752 cm^{-1}) products formed sequentially. After 5.5 h, the reaction was complete, the solution was concentrated to 10 mL, and the product was precipitated with diethyl ether. Purification was effected by overnight Soxhlet extraction with toluene. Slow precipitation at room temperature from a CH_3CN solution layered with Et_2O yielded air-stable red crystals (290 mg, 0.350 mmol, 65%). Anal. Calcd for $C_{38}H_{35}NOP_2AsF_6Mn$: C, 55.2; H, 4.23; N, 1.69. Found: C, 54.6; H, 4.34; N, 1.62.

[(PhC$_6$H$_6$)Mn(NO)(PMe$_3$)$_2$]PF$_6$. [(PhC$_6$H$_6$)Mn(CO)$_2$NO]PF$_6$ (149 mg, 0.338 mmol) was suspended in 50 mL of CH_2Cl_2 at 273 K. Addition of PMe_3 (1.0 mL of a 1.0 M THF solution) led quickly to a clear, bright yellow solution containing the product of nucleophilic addition to the ring (ν_{CO}, ν_{NO} = 2054, 2004, 1764 cm^{-1}). Me_3NO (98 mg, 1.3 mmol, vacuum dried) was added, and the solution slowly turned orange. After 2.5 h, IR spectra indicated a 1:1 mixture of the desired product (1744 cm^{-1}) and (6-*exo*-Ph-5-*exo*-PMe_3-η^4-cyclohexa-1,3-diene)Mn(CO)(NO)PMe_3^+ (1962, 1709 cm^{-1}). Stirring this mixture overnight caused decomposition of the latter species and allowed isolation of the former by filtration, concentration to 5 mL, and precipitation by addition of diethyl ether. Crystal growth by diffusion of Et_2O into a CH_2Cl_2 solution yielded 11.6 mg of analytically pure, air-stable, red product (0.0216 mmol, 6.4%). Anal. Calcd for $C_{18}H_{27}NOP_3F_6Mn$: C, 40.2; H, 5.40; N, 2.61. Found: C, 40.1; H, 5.41; N, 2.38. Attempts to improve the yield were unsuccessful. The major by-product of the reaction proved to be $Mn(NO)_2(PMe_3)_2Cl$.

Collection of NMR Data. The complexes were dissolved in CD_2Cl_2, $CDCl_3$, or 2:1 CD_2Cl_2–CD_3CN and loaded into 5- or 10-mm tubes under argon. Neutral complexes were loaded through a plug of alumina to remove cationic paramagnetic impurities. All NMR spectra were obtained by using a Bruker AM400 instrument. The probe temperature was varied by using a Bruker BVT-1000 temperature control unit. A thermocouple located in the probe under the sample was used to monitor the sample temperature. This measurement is subject to a ±2 K uncertainty. All proton spectra were referenced to an appropriate solvent peak; phosphorus spectra were externally referenced to H_3PO_4, which was designated as 0 ppm.

X-ray Structure of [(6-*exo*-PhC$_6$H$_6$)Mn(NO)dppe]PF$_6$. Orange parallelepiped-shaped crystals suitable for X-ray diffraction were grown at room temperature from a mixture of acetonitrile and diethyl ether. A single crystal of dimensions 0.5 × 0.3 × 0.2 mm was mounted in a glass capillary, and data were collected at 293 K on a Nicolet R3m diffractometer using the θ–2θ technique. Unit cell dimensions were determined from data having 2θ in the range 24–34°. Three standard reflections were monitored every 100 reflections (maximum decay 1.5%). An empirical absorption correction (maximum 0.494, minimum 0.476) was made on the basis of ψ-scan data for six reflections equally distributed throughout the range of 2θ (program XEMP of the SHELXTL 4.1 package[16]). A total of 361 duplicate reflections ($0,k,\pm l$) showed good agreement with R(merge) = 0.0180. The structure was solved by direct methods using the SHELXTL program.[16] Anisotropic refinement of the non-hydrogen atoms utilized the weighting scheme $w = 1/[\sigma(F_o)^2 + 0.00076(F_o)^2]$. The hydrogen atoms were placed in calculated positions with r_{C-H} = 0.96 Å. A summary of X-ray diffraction data is given in Table I. The atomic coordinates and bond lengths and angles are provided in Tables II and III. The atomic numbering scheme is given in Figure 1.

Table I. Summary of X-ray Diffraction Data for [(PhC$_6$H$_6$)Mn(NO)dppe]PF$_6$

complex	[(PhC$_6$H$_6$)Mn(NO)dppe]PF$_6$
formula	$C_{38}H_{35}NOP_3F_6Mn$
fw	783.55
a, Å	11.665 (2)
b, Å	16.961 (6)
c, Å	18.182 (4)
β, deg	95.58 (2)
V, Å^3	3588.4
Z	4
ρ(calcd), g cm^{-3}	1.45
space group	$P2_1/c$ (No. 14)
temp, °C	20
radiation	Mo Kα (0.710 69 Å)
μ, cm^{-1}	5.47
2θ limits, deg	3.5–42
no. of observns	4421
no. of unique data	3477 ($I > 2.5\sigma(I)$)
final no. of variables	451
R	0.039
R_w	0.044
GOF	1.48

Results and Discussion

Complexes with Unidentate Ligands. For those complexes that have structure **3**, we examined six different ligand sets (L, L′, L″) including CO, NO, and/or PMe_3. All of the complexes showed decoalescence of the NMR

(9) Chung, Y. K.; Choi, H. S.; Sweigart, D. A.; Connelly, N. G. *J. Am. Chem. Soc.* **1982**, *104*, 4245. Chung, Y. K.; Honig, E. D.; Robinson, W. T.; Sweigart, D. A.; Connelly, N. G.; Ittel, S. D. *Organometallics* **1983**, *2*, 1479. Chung, Y. K.; Sweigart, D. A.; Connelly, N. G.; Sheridan, J. B. *J. Am. Chem. Soc.* **1985**, *107*, 2388. Pike, R. D.; Sweigart, D. A. *Synlett* **1990**, 564.

(10) Ittel, S. D.; Whitney, J. F.; Chung, Y. K.; Williard, P. G.; Sweigart, D. A. *Organometallics* **1988**, *7*, 1323.

(11) Pike, R. D.; Ryan, W. J.; Carpenter, G. B.; Sweigart, D. A. *J. Am. Chem. Soc.* **1989**, *111*, 8535.

(12) Pike, R. D.; Alavosus, T. J.; Camaioni-Neto, C. A.; Williams, J. C.; Sweigart, D. A. *Organometallics* **1989**, *8*, 2631.

(13) Pike, R. D.; Ryan, W. J.; Lennhoff, N. S.; Van Epp, J.; Sweigart, D. A. *J. Am. Chem. Soc.* **1990**, *112*, 4798.

(14) Connelly, N. G.; Freeman, M. J.; Orpen, A. G.; Sheehan, A. R.; Sheridan, J. B.; Sweigart, D. A. *J. Chem. Soc., Dalton Trans.* **1985**, 1019.

(15) Pike, R. D.; Rieger, A. L.; Rieger, P. H. *J. Chem. Soc., Faraday Trans. 1* **1989**, *85*, 3913.

(16) SHELXTL programs, Nicolet Instrument Co., Madison, WI.

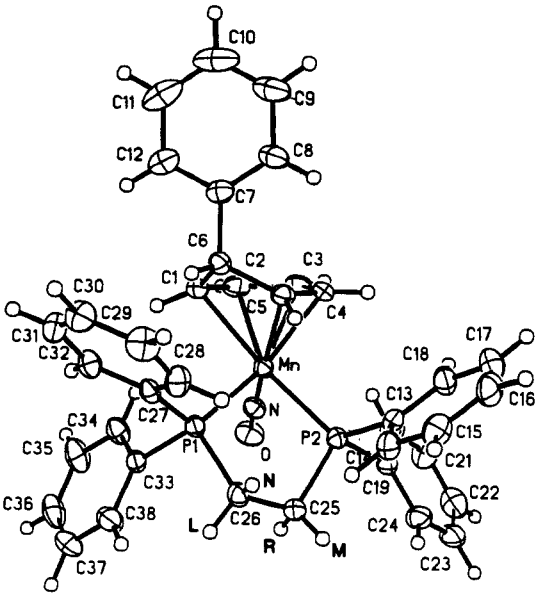

Figure 1. ORTEP drawing of the cation in $[(PhC_6H_6)Mn(NO)dppe]PF_6$ with the thermal ellipsoids at the 50% probability level.

spectra due to slowing cyclohexadienyl ring rotation on the NMR chemical exchange time scale.

The ^1H NMR spectrum (400.137 MHz) of **$[(PhC_6H_6)Mn(CO)_2NO]PF_6$** (**4**) in 2:1 CD_2Cl_2–CD_3CN at 298 K shows four triplets ($^3J_{HH} = {}^3J_{HH} = 6$ Hz) due to the cyclohexadienyl ring protons at δ 6.80 (H3), 6.05 (H2,4), 4.88 (H1,5), and 4.07 (H6) as well as a solvent ($CHDCl_2$) resonance at δ 5.37 (Figure 2). At progressively lower temperatures, the H3 and H6 resonances show no decoalescence but do broaden due to increasingly efficient transverse relaxation (T_2) in a solvent of progressively increasing viscosity. In contrast, the H1,5 signal decoalesces and, at 198 K, is separated into two resonances at δ 4.22 and 5.24 (overlaps solvent resonance; see asterisk in Figure 2). The H2,4 signal also decoalesces and, at 198 K, is clearly separated into two signals of equal area at δ 6.28 and 5.71. After the variation of T_2 values and chemical shifts with temperature was taken into account, the two decoalescences were simulated theoretically as two separate two-site exchanges of magnetization by using computer program DNMR4.[17] The H3, H6, and solvent signals were included in the simulations (Figure 2). Accurate line fitting required equal rates for the two different decoalescences; i.e., they both reflect the same rate process. At 198 K, the spectrum is still exchange-broadened and accurate simulation requires a rate constant of 20 s^{-1}. Using Eyring transition state theory, the activation parameters for the observed rate process can be calculated ($\Delta H^\ddagger = 9.9 \pm 0.4$ kcal mol^{-1}, $\Delta S^\ddagger = -2 \pm 4$ cal mol^{-1} K^{-1}; $\Delta G^\ddagger = 10.4 \pm 0.2$ kcal mol^{-1} at 234 K). While one must be wary of undetermined systematic errors in DNMR line-shape analyses, we did take care to account for T_2 and chemical shift variations with temperature and feel confident about the accuracy of the activation parameters above. In particular, the small $\Delta S^\ddagger$ value is consistent with an intramolecular conformational exchange rate process and inconsistent with a process that involves ligand dissociation or molecular association. Indeed, for all the complexes of interest in this paper, all $\Delta S^\ddagger$ values extracted from DNMR line-shape analyses have absolute values less than 4 cal mol^{-1} K^{-1} consistent with intramolecular exchange processes.

(17) Bushweller, C. H.; Letendre, L. J.; Brunelle, J. A.; Bilofsky, H. S.; Whalon, M. R.; Fleischman, S. H. Quantum Chemistry Program Exchange (Indiana University), 1983, No. 466.

Table II. Atom Coordinates ($\times 10^4$) and Temperature Factors (Å $\times 10^3$) for $[(PhC_6H_6)Mn(NO)dppe]PF_6$

atom	*x*	*y*	*z*	U^a
Mn	3106 (1)	8703 (1)	3877 (1)	35 (1)
P(1)	4346 (1)	7645 (1)	3885 (1)	37 (1)
P(2)	1980 (1)	7880 (1)	4517 (1)	37 (1)
P(3)	2078 (1)	4294 (1)	3008 (1)	69 (1)
C(1)	3940 (3)	9200 (2)	2917 (2)	45 (1)
C(2)	3396 (3)	9772 (2)	3302 (2)	52 (1)
C(3)	2212 (3)	9706 (2)	3388 (1)	53 (1)
C(4)	1635 (3)	9023 (2)	3135 (2)	48 (1)
C(5)	2232 (3)	8450 (2)	2769 (2)	43 (1)
C(6)	3225 (3)	8714 (2)	2356 (2)	42 (1)
C(7)	2906 (3)	9170 (2)	1640 (2)	48 (1)
C(8)	1781 (3)	9279 (2)	1349 (2)	61 (1)
C(9)	1534 (5)	9690 (3)	689 (2)	84 (2)
C(10)	2400 (5)	9990 (2)	331 (2)	95 (2)
C(11)	3519 (5)	9894 (2)	610 (2)	90 (2)
C(12)	3785 (4)	9475 (2)	1268 (2)	68 (2)
C(13)	772 (3)	7356 (2)	4037 (2)	40 (1)
C(14)	819 (3)	6565 (2)	3838 (2)	50 (1)
C(15)	−133 (3)	6198 (2)	3481 (2)	63 (1)
C(16)	−1133 (3)	6602 (3)	3322 (2)	69 (1)
C(17)	−1196 (3)	7391 (3)	3506 (2)	70 (2)
C(18)	−253 (3)	7759 (2)	3867 (2)	54 (1)
C(19)	1352 (3)	8307 (2)	5303 (2)	42 (1)
C(20)	1239 (3)	9110 (2)	5381 (2)	60 (1)
C(21)	796 (4)	9428 (3)	5993 (2)	78 (2)
C(22)	464 (4)	8949 (3)	6530 (2)	74 (2)
C(23)	542 (3)	8155 (3)	6459 (2)	71 (2)
C(24)	981 (3)	7825 (2)	5844 (2)	61 (1)
C(25)	2961 (3)	7127 (2)	4940 (2)	44 (1)
C(26)	3747 (3)	6822 (2)	4383 (2)	46 (1)
C(27)	4707 (3)	7214 (2)	3021 (2)	38 (1)
C(28)	3967 (3)	6686 (2)	2625 (2)	53 (1)
C(29)	4194 (3)	6440 (2)	1936 (2)	65 (1)
C(30)	5136 (3)	6707 (2)	1620 (2)	61 (1)
C(31)	5871 (3)	7225 (2)	2002 (2)	57 (1)
C(32)	5666 (3)	7475 (2)	2698 (2)	48 (1)
C(33)	5737 (2)	7863 (2)	4400 (2)	39 (1)
C(34)	6172 (3)	8618 (2)	4411 (2)	57 (1)
C(35)	7218 (3)	8799 (3)	4801 (2)	72 (2)
C(36)	7821 (3)	8229 (3)	5202 (2)	73 (2)
C(37)	7409 (3)	7478 (3)	5194 (2)	76 (2)
C(38)	6376 (3)	7291 (2)	4793 (2)	64 (1)
N	3660 (2)	9073 (1)	4675 (1)	41 (1)
O	4022 (2)	9354 (2)	5243 (1)	63 (1)
F(1)	1844 (3)	3374 (2)	2992 (2)	132 (2)
F(2)	3119 (3)	4132 (2)	3602 (2)	151 (2)
F(3)	2260 (3)	5194 (2)	3032 (2)	146 (2)
F(4)	1290 (3)	4358 (2)	3659 (2)	126 (1)
F(5)	2863 (4)	4209 (2)	2387 (2)	167 (2)
F(6)	965 (3)	4406 (2)	2459 (2)	128 (1)

[a] Equivalent isotropic *U* defined as one-third of the trace of the orthogonalized U_{ij} tensor.

The spectrum of **4** at 198 K reveals six diastereotopic cyclohexadienyl ring protons consistent with a molecular conformation that has C_1 symmetry. The 198 K spectrum is rationalized best in terms of a strong preference for the two enantiomeric conformations **5** and **6** (eq 1; X = CO, Y = NO). In **5** or **6**, all six ring protons are diastereotopic.

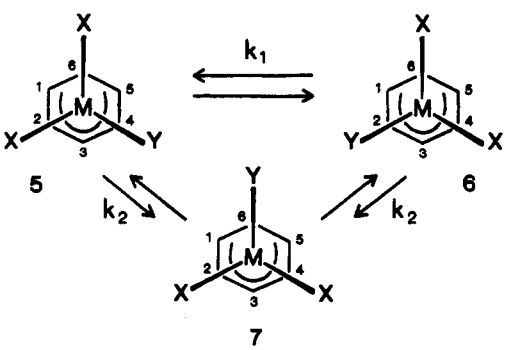

(1)

Table III. Bond Lengths (Å) and Angles (deg) for [(PhC$_6$H$_6$)Mn(NO)dppe]PF$_6$

Bond Lengths

Mn–P1	2.304 (1)	C19–C24	1.381 (5)	C1–C6	1.500 (4)
Mn–C1	2.242 (3)	C21–C22	1.355 (6)	C3–C4	1.395 (5)
Mn–C3	2.143 (3)	C23–C24	1.391 (5)	C5–C6	1.507 (5)
Mn–C5	2.209 (3)	C27–C28	1.395 (4)	C7–C8	1.379 (5)
P1–C26	1.838 (3)	C28–C29	1.371 (5)	C8–C9	1.393 (5)
P1–C33	1.831 (3)	C30–C31	1.369 (5)	C10–C11	1.363 (7)
P2–C19	1.818 (3)	C33–C34	1.376 (5)	C13–C14	1.391 (5)
P3–F1	1.584 (3)	C34–C35	1.386 (5)	C14–C15	1.380 (5)
P3–F3	1.541 (3)	C36–C37	1.362 (7)	C16–C17	1.383 (6)
P3–F5	1.527 (4)	N–O	1.177 (3)	C19–C20	1.376 (5)
C1–C2	1.385 (5)	Mn–P2	2.306 (1)	C20–C21	1.382 (6)
C2–C3	1.409 (5)	Mn–C2	2.136 (3)	C22–C23	1.356 (6)
C4–C5	1.399 (5)	Mn–C4	2.147 (3)	C25–C26	1.521 (5)
C6–C7	1.528 (4)	Mn–N	1.654 (2)	C27–C32	1.384 (5)
C7–C12	1.382 (5)	P1–C27	1.817 (3)	C29–C30	1.366 (6)
C9–C10	1.353 (7)	P2–C13	1.817 (3)	C31–C32	1.377 (5)
C11–C12	1.400 (5)	P2–C25	1.833 (3)	C33–C38	1.381 (5)
C13–C18	1.385 (4)	P3–F2	1.570 (3)	C35–C36	1.363 (6)
C15–C16	1.359 (5)	P3–F4	1.570 (3)	C37–C38	1.383 (5)
C17–C18	1.376 (5)	P3–F6	1.571 (3)		

Bond Angles

P1–Mn–P2	85.0	C9–C10–C11	120.6 (4)	F1–P3–F3	177.9 (2)
P2–Mn–C1	158.5 (1)	C7–C12–C11	119.6 (4)	F1–P3–F4	88.3 (2)
P2–Mn–C2	152.3 (1)	P2–C13–C18	118.6 (2)	F3–P3–F4	90.0 (2)
P1–Mn–C3	154.3 (1)	C13–C14–C15	120.5 (3)	F2–P3–F5	90.7 (2)
C1–Mn–C3	67.0 (1)	C15–C16–C17	120.0 (4)	F4–P3–F5	178.2 (2)
P1–Mn–C4	131.6 (1)	C13–C18–C17	121.0 (3)	F2–P3–F6	174.5 (2)
C1–Mn–C4	78.2 (1)	P2–C19–C24	120.2 (3)	F4–P3–F6	87.9 (2)
C3–Mn–C4	38.0 (1)	C19–C20–C21	121.2 (3)	Mn–C1–C2	67.4 (2)
P2–Mn–C5	96.2 (1)	C21–C22–C23	120.0 (4)	C2–C1–C6	118.4 (3)
C2–Mn–C5	78.4 (1)	C19–C24–C23	120.0 (4)	Mn–C2–C3	71.0 (2)
C4–Mn–C5	37.4 (1)	P1–C26–C25	110.6 (2)	Mn–C3–C2	70.5 (2)
P2–Mn–N	88.9 (1)	P1–C27–C32	120.1 (2)	C2–C3–C4	118.4 (3)
C2–Mn–N	92.3 (1)	C27–C28–C29	120.1 (3)	Mn–C4–C5	73.7 (2)
C4–Mn–N	132.6 (1)	C29–C30–C31	119.3 (3)	Mn–C5–C4	68.9 (2)
Mn–P1–C26	109.0 (1)	C27–C32–C31	120.7 (3)	C4–C5–C6	118.1 (3)
C26–P1–C27	104.5 (1)	P1–C33–C38	122.0 (2)	C1–C6–C7	112.1 (3)
C26–P1–C33	105.2 (1)	C33–C34–C35	121.3 (3)	C6–C7–C8	122.6 (3)
Mn–P2–C13	120.4 (1)	C35–C36–C37	119.6 (4)	C8–C7–C12	119.0 (3)
C13–P2–C19	102.7 (1)	C33–C38–C37	120.7 (4)	C8–C9–C10	120.0 (4)
C13–P2–C25	106.6 (1)	P1–Mn–C1	88.7 (1)	C10–C11–C12	120.2 (4)
F1–P3–F2	87.7 (2)	P1–Mn–C2	122.3 (1)	P2–C13–C14	123.2 (2)
F2–P3–F3	93.4 (2)	C1–Mn–C2	36.8 (1)	C14–C13–C18	118.2 (3)
F2–P3–F4	87.9 (2)	P2–Mn–C3	114.3 (1)	C14–C15–C16	120.5 (4)
F1–P3–F5	90.4 (2)	C2–Mn–C3	38.5 (1)	C16–C17–C18	119.7 (3)
F3–P3–F5	91.3 (2)	P2–Mn–C4	90.6 (1)	P2–C19–C20	121.7 (3)
F1–P3–F6	88.7 (2)	C2–Mn–C4	68.4 (1)	C20–C19–C24	118.1 (3)
F3–P3–F6	90.1 (2)	P1–Mn–C5	95.1 (1)	C20–C21–C22	120.0 (4)
F5–P3–F6	93.4 (2)	C1–Mn–C5	63.9 (1)	C22–C23–C24	120.6 (4)
Mn–C1–C6	93.9 (2)	C3–Mn–C5	67.2 (1)	P2–C25–C26	110.4 (2)
Mn–C2–C1	75.8 (2)	P1–Mn–N	95.6 (1)	P1–C27–C28	121.3 (2)
C1–C2–C3	120.1 (3)	C1–Mn–N	112.2 (1)	C28–C27–C32	118.2 (3)
Mn–C3–C4	71.2 (2)	C3–Mn–N	101.3 (1)	C28–C29–C30	121.2 (3)
Mn–C4–C3	70.9 (2)	C5–Mn–N	168.5 (1)	C30–C31–C32	120.5 (3)
C3–C4–C5	119.1 (3)	Mn–P1–C27	120.4 (1)	P1–C33–C34	120.2 (2)
Mn–C5–C6	95.0 (2)	Mn–P1–C33	111.8 (1)	C34–C33–C38	117.8 (3)
C1–C6–C5	103.1 (2)	C27–P1–C33	104.8 (1)	C34–C35–C36	120.0 (4)
C5–C6–C7	116.1 (3)	Mn–P2–C19	116.6 (1)	C36–C37–C38	120.6 (4)
C6–C7–C12	118.4 (3)	Mn–P2–C25	105.7 (1)	Mn–N–O	177.6 (2)
C7–C8–C9	120.5 (4)	C19–P2–C25	103.3 (1)		

The C_s-symmetric species **7**, which would show only four ring proton resonances, is present at too low a concentration to be detectable. In the preferred conformations (**5** and **6**), C6 of the cyclohexadienyl ring eclipses CO. The NO ligand eclipses one of the carbons (C4 in **5**; C2 in **6**) in the π-system of the cyclohexadienyl ring.

The DNMR behavior shown in Figure 2 reflects exchange between enantiomers **5** and **6**. H1 and H5, as well as H2 and H4, exchange between diastereotopic sites while the environments of H3 and H6 remain unchanged, as reflected by the DNMR spectra in Figure 2. The exchange can occur by a direct path (k_1 in eq 1), via **7** (k_2 in eq 1), or via both pathways. In the absence of any detectable concentration of **7**, the DNMR spectra in Figure 2 do not allow an elucidation of the itinerary for exchange. Indeed, it is not possible to determine whether **7** is an unstable intermediate or a transition state. It is likely that exchange occurs by both pathways and the derived activation parameters probably reflect a composite of the two different itineraries (vide infra).

^{1}H NMR data at room temperature and at or near the slow-exchange temperature for **4** and five other unidentate complexes are compiled in Table IV. Cyclohexadienyl ring rotation barriers ($\Delta G^{\ddagger}$) and conformational preferences are summarized in Table V.

The ^{1}H NMR spectrum (400.132 MHz) of **[(PhC$_6$HMe$_5$)Re(CO)$_2$NO]PF$_6$ (8)** in CD_2Cl_2 at 297 K shows three methyl singlets at δ 3.01 (Me3), 2.56 (Me2,4),

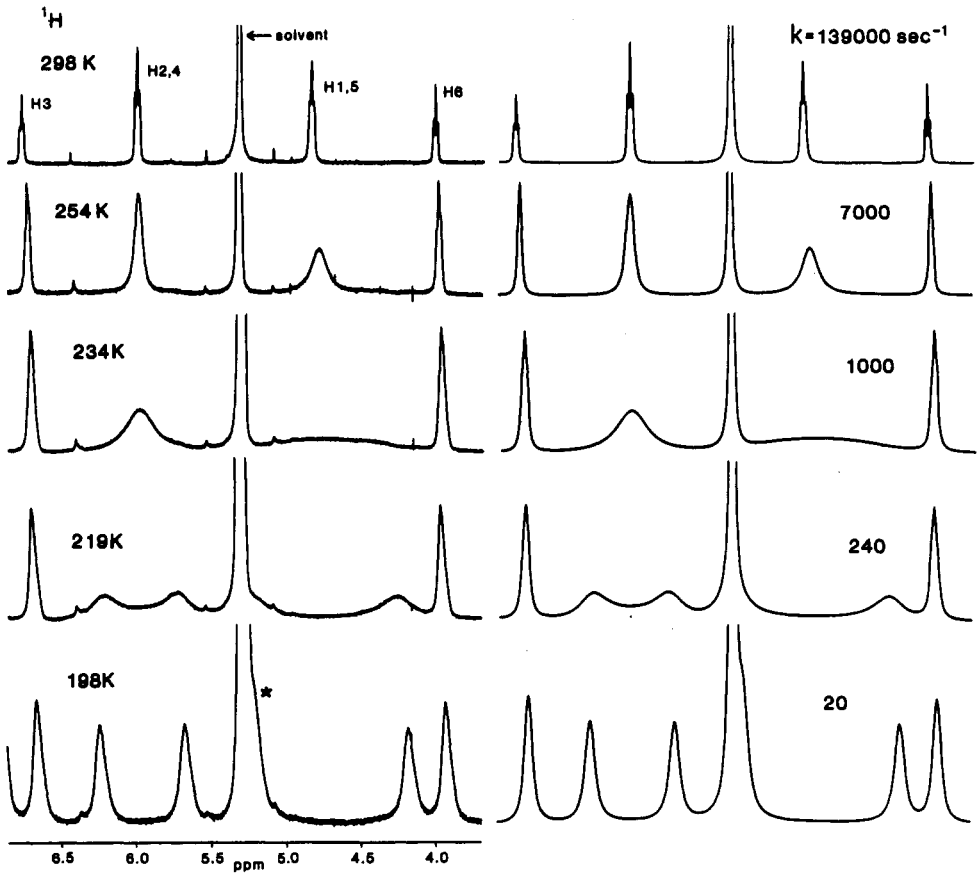

Figure 2. ^{1}H DNMR spectra (400.137 MHz) of the cyclohexadienyl ring protons of $[(PhC_6H_6)Mn(CO)_2NO]PF_6$ (4) in 2:1 CD_2Cl_2–CD_3CN. The rate constant k is associated with interconversion between the C_1-symmetric enantiomers 5 and 6 in eq 1.

Table IV. ^{1}H NMR Data for Cyclohexadienyl Complexes with Unidentate Ligands[a]

complex	temp, K	^{1}H NMR, δ (J, Hz)
$[(PhC_6H_6)Mn(CO)_2NO]PF_6$ (4)	298	7.1 (m, Ph), 6.80 (t, J = 5.5, H3), 6.05 (t, J = 6.3, H2,4), 4.88 (t, J = 5.7, H1,5), 4.07 (t, J = 6.0, H6)[b]
	198	7.1 (m, Ph), 6.64 (H3), 6.28 (H2 or H4), 5.71 (H4 or 2), 5.24 (H1), 4.22 (H5), 3.92 (H6)[b,d]
$[(PhC_6HMe_5)Mn(CO)_2NO]PF_6$	297	7.1 (m, Ph), 3.92 (H6), 2.78 (Me3), 2.25 (Me2,4), 2.02 (Me1,5)
	183	7.1 (m, Ph), 3.83 (H6), 2.69 (Me3), 2.25 (Me2 or 4), 2.12 (Me4 or 2, Me1), 1.81 (Me5)
$[(PhC_6HMe_5)Re(CO)_2NO]PF_6$ (8)	297	7.1 (m, Ph), 4.27 (H6), 3.01 (Me3), 2.56 (Me2,4), 2.25 (Me1,5)
	188	7.1 (m, Ph), 4.19 (H6), 2.91 (Me3), 2.57 (Me2 or 4), 2.43 (Me4 or 2), 2.39 (Me1), 1.99 (Me5)
$[(PhC_6H_6)Mn(NO)(PMe_3)_2]PF_6$	296	7.25, 7.04 (m, d, J = 7.8, Ph), 5.85 (tt, J = 5.8, 1.3, H3), 5.28 (t, J = 5.5, H2,4), 3.76 (br, H1,5), 3.43 (t, J = 5.9, H6), 1.69 (d, J = 9.7, Me)[c]
	213	7.1 (m, Ph), 5.85 (H3), 5.29 (H2 or 4), 5.22 (H4 or 2), 4.29 (H1), 3.36 (H6), 3.04 (H5), 1.87 (Me), 1.43 (Me)
$(PhC_6H_6)Mn(CO)_2PMe_3$	293	7.1 (m, Ph), 5.46 (tt, J = 6.4, 1.5, H3), 4.58 (q, J = 5.2, H2,4), 3.73 (t, J = 6.0, H6), 3.09 (td, J = 6.0, 1.1, H1,5), 1.29 (d, J = 8.5, Me)
	183	7.1 (m, Ph), 5.43 (H3), 4.64 (H2 or 4), 4.41 (H4 or 2), 3.69 (H6), 3.22 (H1 or 5), 2.87 (H5 or 1), 1.17 (Me)[d]
$(PhC_6H_6)Mn(CO)(PMe_3)_2$	296	7.1 (m, Ph), 4.90 (H3), 4.38 (H2,4), 3.40 (H6), 2.52 (H1,5), 1.43 (Me)
	198	7.1 (m, Ph), 4.80 (H3), 4.43 (H2 or 4), 4.25 (H4 or 2), 3.34 (H6), 2.43 (H1,5), 1.64 (Me), 1.08 (Me)

[a] In CD_2Cl_2; singlet unless noted. The numbering scheme for PF_6^- salts corresponds to structure 1 with L = NO. [b] In 2:1 CD_2Cl_2–CD_3CN. [c] Fast exchange not reached. [d] Slow exchange not reached.

and 2.25 (Me1,5) as shown in Figure 3. The minor peaks in the 297 K spectrum are due to an impurity and remain sharp down to 198 K. At lower temperatures in a manner strictly analogous to that for 4, the Me3 signal shows no decoalescence while each of the Me2,4 and Me1,5 signals decoalesces into two singlets of equal area (Table IV). At 198 K, the Me2,4 and Me1,5 singlets are broadened relative to the Me3 signal due to a small rate of exchange. The 198 K spectrum reveals an essentially exclusive preference for enantiomeric conformations analogous to 5 and 6 (eq 1). In the preferred conformations, the cyclohexadienyl C6 carbon eclipses a CO ligand. Activation parameters for the enantiomerization include a small $\Delta S^\ddagger$ value (-1 ± 4 cal mol^{-1} K^{-1}) with $\Delta H^\ddagger = 10.6 \pm 0.4$ kcal mol^{-1} and $\Delta G^\ddagger = 10.7 \pm 0.2$ kcal mol^{-1} at 223 K.

Four other complexes with a set of three unidentate ligands (3; L, L′, L″) show strictly analogous ^{1}H DNMR behavior (Table IV). Each of these complexes exhibits decoalescence of ^{1}H NMR signals due to protons or methyl groups on C1,5 and C2,4. The only exception is $(PhC_6H_6)Mn(CO)(PMe_3)_2$, which does not show H1,5 decoalescence. Apparently, this is due to coincidental chemical shift overlap at slow exchange, because both H2,4 and the $(PMe_3)_2$ signals decoalesce. Conformational preferences for all these complexes are summarized in Table V.

Table V. Detectable Equilibrium Conformations and Cyclohexadienyl Ring Rotational Barriers

complex	equilib conformns	$\Delta G^{\ddagger}$, kcal mol^{-1} [a]
$[(PhC_6H_6)Mn(CO)_2NO]PF_6$	100% **5** and **6** (eq 1; X = CO, Y = NO)	10.4
$[(PhC_6HMe_5)Mn(CO)_2NO]PF_6$	100% **5** and **6** (eq 1; X = CO, Y = NO)[b]	10.7
$[(PhC_6HMe_5)Re(CO)_2NO]PF_6$	100% **5** and **6** (eq 1; X = CO, Y = NO)[b]	10.7
$[(PhC_6H_6)Mn(NO)(PMe_3)_2]PF_6$	100% **5** and **6** (eq 1; X = PMe_3, Y = NO)	11.4
$(PhC_6H_6)Mn(CO)_2PMe_3$	100% **5** and **6** (eq 1; X = CO, Y = PMe_3)	9.2
$(PhC_6H_6)Mn(CO)(PMe_3)_2$	100% **5** and **6** (eq 1; X = PMe_3, Y = CO)	10.8
$(C_6H_7)Mn(CO)(eptb)_2$	100% C_1-symmetric enantiomers (eptb eclipses C6)[c]	9.8[d]
$[(PhC_6H_6)Mn(NO)dppen]PF_6$	100% **10** (see text) and its enantiomer	12.6
$[(PhC_6H_6)Mn(NO)dppe]PF_6$	98% **13** and **14** (eq 2; Y = NO);	12.9 (**13** to **14**)[e]
	2% **15**; at 199 K	12.4 (**13** or **14** to **15**)[e]
$(PhC_6H_6)Mn(CO)dppe$	65% **13** and **14** (eq 2; Y = CO);	11.1 (**13** to **14**)[d]
	35% **15**; at 183 K	10.0 (**13** or **14** to **15**)[d]
$[(PhC_6H_6)Mn(NO)arphos]PF_6$	88% **20** (see text); 12% **21**; at 231 K	12.1 (**21** to **20**)[e]

[a] From ^{1}H DNMR data, except as noted. $\Delta G^{\ddagger}$ values are approximately independent of temperature and have an estimated error of ±0.2 kcal/mol. [b] Cyclohexadienyl ring is 1,2,3,4,5-pentamethyl-substituted. [c] Reference 8; cyclohexadienyl ring has no 6-phenyl substituent. [d] From $^{31}P\{^1H\}$ DNMR. [e] From ^{1}H and $^{31}P\{^1H\}$ DNMR.

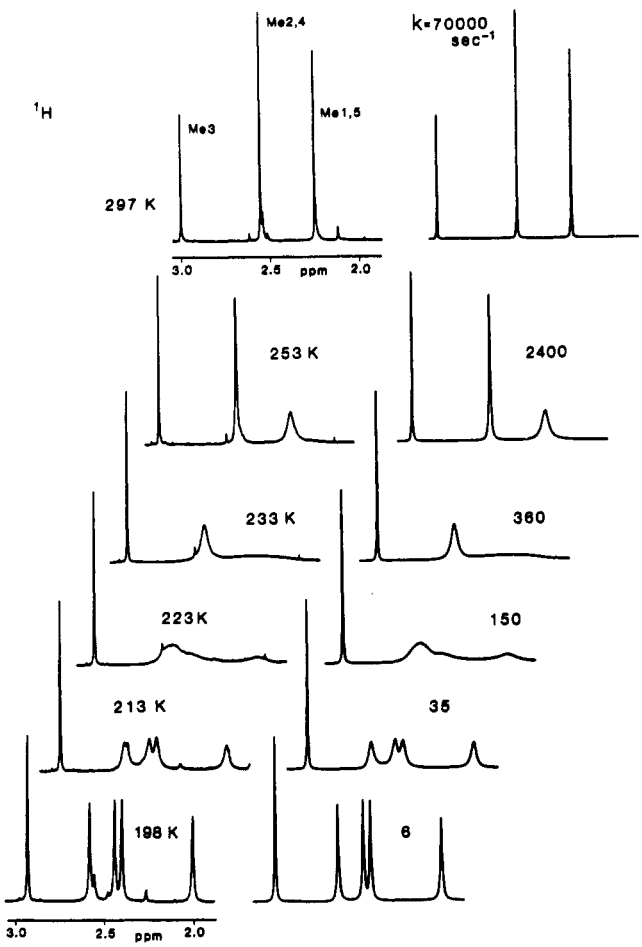

Figure 3. ^{1}H DNMR spectra (400.137 MHz) of the pentamethyl groups of $[(PhC_6HMe_5)Re(CO)_2NO]PF_6$ (**8**) in CD_2Cl_2. The rate constant k is associated with interconversion between the C_1-symmetric enantiomers **5** and **6** in eq 1 (the ring is 1,2,3,4,5-pentamethyl-substituted).

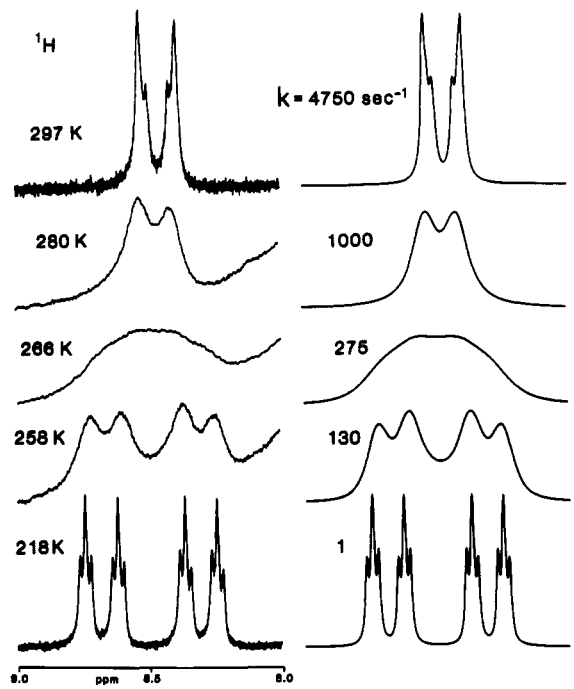

Figure 4. ^{1}H DNMR spectra (400.137 MHz) of the alkenyl protons of $[(PhC_6H_6)Mn(dppen)NO]PF_6$ (**9**) in CD_2Cl_2. The rate constant k is associated with interconversion between **10** and its enantiomer.

For all of the complexes in Table IV, two of the unidentate ligands are identical and the third is different. In each case, the slow-exchange ^{1}H NMR spectrum shows a strong preference for the C_1-symmetric enantiomeric conformations (e.g., **5** and **6**) and undetectable amounts of the C_s-symmetric species (e.g., **7**). The clear trend is that C6 of the cyclohexadienyl ring eclipses one of the two identical ligands while the unique ligand eclipses a carbon in the cyclohexadienyl π-system. In the preferred conformations, a nitrosyl ligand invariably eclipses a carbon in the cyclohexadienyl π-system, probably for electronic reasons. This conformational preference for the nitrosyl ligand is also found in the X-ray structures of $[(MeC_6H_6)Mn(CO)_2NO]PF_6$[10] and $[(PhC_6H_6)Mn(NO)dppe]PF_6$ (Figure 1). When all three unidentate ligands are different, as in $[(PhC_6H_6)Mn(CO)(NO)PR_3]PF_6$, X-ray studies again show that, in the crystal, the preferred conformation is the eclipsed structure (**1**) with the nitrosyl ligand eclipsing a carbon in the cyclohexadienyl π-system.[11,13,18] Extended Hückel molecular orbital calculations for $[(C_6H_7)Mn(CO)_2NO]^+$ do indicate that energy is minimized for those conformations in which NO eclipses C2 or C4 of the cyclohexadienyl ring (as in **6** or **5** in eq 1).[19]

Table V shows that the rotation barrier is only modestly dependent on the particular set of unidentate ligands. Changing the metal from manganese to rhenium or methylating the cyclohexadienyl ring leads to no change in $\Delta G^{\ddagger}$. Replacing a CO ligand by PMe_3 increases $\Delta G^{\ddagger}$, while replacing NO^+ with CO or PMe_3 decreases $\Delta G^{\ddagger}$.

Complexes with Bidentate Ligands. Four PhC_6H_6 complexes of manganese, each having a bidentate ligand,

(18) Pike, R. D.; Ryan, W. J.; Sweigart, D. A. To be submitted for publication.
(19) Alavosus, T. J.; Sweigart, D. A. Unpublished results.

Table VI. ^{1}H NMR Data for (Cyclohexadienyl)manganese Complexes with Bidentate Ligands

complex	temp, K	chem shift, ppm (multiplicity, J (Hz), assignt)
$[(PhC_6H_6)Mn(NO)dppen]PF_6$ (9)[a]	298	8.46 (m, CHCH), 7.3 (m, Ph, dppen), 7.07, 6.48 (m, d, J = 4.2, Ph6), 6.81 (t, J = 5.7, H3), 5.19 (br, H2,4), 3.25 (br, H1,5), 1.90 (t, J = 5.9, H6)[b]
	218	8.67, 8.30 (ddd, ddd, J = 49, 10, 8, CHCH), 7.6 (m, Ph, dppen), 7.02, 6.39 (m, m, Ph6), 6.91 (br t, J = 5.4, H3), 5.53 (t, J = 5.8, H2 or 4), 4.81 (m, H4 or 2, H1), 1.54 (t, J = 5.1, H6), 1.43 (H5)
$[(PhC_6H_6)Mn(NO)dppe]PF_6$ (12)[c]	303	7.5 (m, Ph, dppe), 7.03, 6.47 (m, m, Ph6), 6.61 (H3), 5.10 (H2,4), 3.53 (m, CH_2CH_2), 3.0 (br, H1,5), 1.55 (H6)[b]
	198	dominant subspectrum (also see text and Table VII)[d] 7.5 (m, Ph, dppe), 7.02, 6.36 (m, m, Ph6), 6.81 (H3), 5.46 (H2 or 4), 5.00 (H4 or 2), 4.47 (H1), 1.45 (H5, 6); CH_2CH_2 3.91 (d, J = 38), 3.67 (d, J = 38), 3.52, 2.12
$(PhC_6H_6)Mn(CO)dppe$ (18)[a]	293	7.4 (m, Ph, dppe), 7.06, 6.76 (m, m, Ph6), 5.63 (H3), 4.42 (H2,4), 2.94 (H6), 2.36 (m, H1,5, CH_2CH_2)
	183	complex spectrum (see text and also Table VIII)[e]
$[(PhC_6H_6)Mn(NO)arphos]PF_6$ (19)	308	7.5 (m, Ph, arphos), 7.07, 6.50 (m, m, Ph6), 6.72 (t, J = 5.3, H3), 5.32 (t, J = 5.9, H2), 5.17 (q, J = 5.9, H4), 4.3 (br, H1), 3.5 (m, CH_2CH_2), 1.7 (br, H5), 2.22 (t, J = 5.7, H6)[b]
	228	complex spectrum consisting of a dominant subspectrum (90% **20**) superimposed upon a minor subspectrum (10% **21**) (see text, Table IX, and Figure 8)

[a] In CD_2Cl_2; singlet unless noted. [b] Fast exchange not reached. [c] In $CDCl_3$. [d] **12** exists as a 98% mixture of **13** and **14** (eq 2; Y = NO) and 2% of **15**. [e] **18** exists as a mixture of enantiomers **13** and **14** (65%) and **15** (35%; eq 2; Y = CO).

were studied. The four ligand sets include dppen and NO, dppe and NO, dppe and CO, and arphos and NO.

The ^{1}H NMR spectrum (400.137 MHz) of **$[(PhC_6H_6)Mn(dppen)NO]PF_6$ (9)** in CD_2Cl_2 at 297 K shows one second-order multiplet at δ 8.46 for the alkenyl protons of the dppen ligand (Figure 4). The multiplet reflects magnetic nonequivalence and exchange of magnetization within the PCH=CHP four-spin system. At lower temperatures, the multiplet decoalesces and is sharpened into two apparent doublets of triplets at 218 K (Figure 4). The spectrum at 218 K is simulated adequately by using two different proton chemical shifts at δ_A 8.68 and δ_B 8.30 as part of an ABXY spin system (A = B = ^{1}H; X = Y = ^{31}P; J_{AB} = 8 Hz, J_{AX} = 48, J_{AY} = 10, J_{BX} = 10, J_{BY} = 48, J_{XY} = 4). The spectrum at 218 K is consistent with a strong preference for conformation **10** and its enantiomer, in

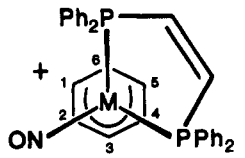

10

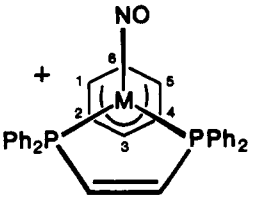

11

which the alkenyl protons are diastereotopic. There is no evidence in the spectrum for the C_s-symmetric species **11** that will show identical chemical shifts for the enantiotopic alkenyl protons. The conformational preference in **9** is highly analogous to that in the other complexes discussed above. Adequate simulations of the DNMR spectra were achieved by using an ABXY to BAYX magnetization exchange model ($\Delta G^{\ddagger}$ = 12.6 ± 0.2 kcal mol^{-1} at 266 K). The observed process involves exchange between **10** and its enantiomer. Since resonances due to **11** are not observed, no conclusions can be drawn regarding the role of **11** in the exchange process.

At 297 K, the ^{1}H NMR spectrum of the cyclohexadienyl ring protons of **9** shows two sharp triplets at δ 6.80 (H3) and 1.90 (H6), a slightly exchange-broadened singlet at δ 5.18 (H2,4), and a severely exchange-broadened H1,5 resonance centered approximately at δ 3.25. The H1,5 signal is essentially collapsed into the base line. At lower temperatures the H3 and H6 resonances show no evidence of decoalescence while the H1,5 and H2,4 signals each decoalesce into two resonances of equal area. At 218 K, the cyclohexadienyl ring shows six sharp proton resonances at δ 6.91 (H3), 5.53 (H2 or H4), 4.82 (H2 or H4), 4.82 (H1 or H5), 1.55 (H6), and 1.44 (H1 or H5). Two of the signals are superimposed. The lack of any decoalescence for the H3 and H6 signals and the observation of just six ring proton signals at 218 K reveal again a strong preference for **10** and its enantiomer. From simulations of the dynamic H1,5 and H2,4 resonances, the $\Delta G^{\ddagger}$ values for both exchanges of magnetization at 266 K are equal at 12.6 ± 0.2 kcal mol^{-1} and identical with that derived from the DNMR spectra of the alkenyl protons. The spectra of both the alkenyl and cyclohexadienyl protons decoalesce in response to the same rate process, i.e., cyclohexadienyl ring rotation that exchanges **10** and its enantiomer. NMR parameters for **9** are compiled in Table VI.

The crystal and molecular structure of **$[(PhC_6H_6)Mn(dppe)NO]PF_6$ (12)** has been determined by using X-ray crystallography (see Experimental Section and Figure 1). Pertinent diffraction data, atomic coordinates, bond lengths, and bond angles are given in Tables I–III. The Mn–N–O bond angle is 177.6 (2)° with the nitrosyl ligand eclipsing C2 of the cyclohexadienyl ring (Figure 1). The cyclohexadienyl C4 and C6 atoms respectively eclipse the P2 and P1 atoms. The relatively electron-rich dppe ligand induces Mn–N and N–O bond lengths substantially shorter and longer, respectively, than those in $[(MeC_6H_6)Mn(CO)_2NO]PF_6$.[10] The dienyl region of the cyclohexadienyl ring is essentially planar with C6 out of plane. The five-membered metallacycle adopts a classic envelope conformation. C26, P1, Mn, and P2 are essentially coplanar. The C26–P1–Mn–P2 dihedral angle is equal to 0.9°. C25 is out of plane at the tip of the flap of the open envelope. The P1–Mn–P2–C25 dihedral angle is 22.3°. The molecular conformation of the cation in Figure 1 is represented schematically by structure **13** (Y = NO) in eq 2.

The ^{1}H NMR spectrum of **12** in $CDCl_3$ at 303 K shows relatively sharp cyclohexadienyl ring signals at δ 6.61 (H3), 5.10 (H2,4), and 2.00 (H6) as well as a doublet at δ 6.48 (J = 7 Hz) due to the ortho protons on the *exo*-phenyl group bonded to C6 of the cyclohexadienyl ring. Between δ 2.50 and 4.00, the spectrum shows significantly exchange-broadened resonances due to the PCH_2CH_2P moiety (δ 3.53, 3.02) and H1,5 of the cyclohexadienyl ring (very broad signal centered at δ 3.34). A signal due to water (δ 1.56) progressively decreases in intensity at lower temperatures due presumably to crystallization and, at 198 K, is absent from the spectrum. A portion of the spectrum at various temperatures is shown in Figure 5. At temperatures below 303 K, the H3 resonance does not show

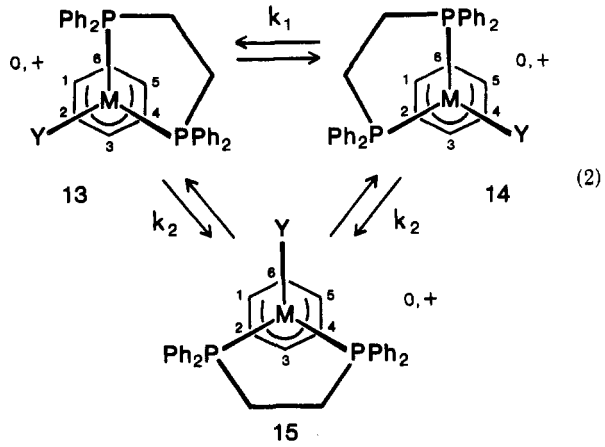

(2)

any discernible evidence of a decoalescence. From 303 K to about 240 K, the behavior of the H6 signal is obscured by the water resonance. In contrast, the H2,4 resonance decoalesces and, at 198 K, is separated into two signals at δ 5.47 and 5.01 (Figure 5). The H1,5 signal also decoalesces and, at 198 K, is split into two signals at δ 4.47 and 1.44. The resonance at δ 1.44 overlaps the signal due to H6 (δ 1.42). The water signal is apparently absent from the 198 K spectrum. The PCH_2CH_2P subspectrum also undergoes a complex decoalescence (Figure 5).

The behavior of the H2,4 resonance is salient. At 262 K (Figure 5), separation into two exchange-broadened signals is evident with more peak area under the lower frequency maximum. At progressively lower temperatures (e.g., 252 and 243 K), the differentially greater area under the lower frequency signal is clearly evident (see asterisks on the 243 K spectrum in Figure 5). In the slow-exchange spectrum at 198 K, the resonance at δ 5.01 has a smaller peak height but a greater width at half-height and a peak area larger by 2–4% than the higher frequency resonance at δ 5.47. At 198 K, the signal at δ 5.47 is simulated adequately as an unresolved triplet (J_{HH} = J_{HH} = 6 Hz). Simulation of the signal at δ 5.01 can be achieved by superimposing an unresolved quartet (J_{HH} = J_{HH} = J_{HP} = 6 Hz) that has an area equal to the peak at δ 5.47 upon a very low intensity (2–4%), narrow multiplet that could be a triplet or a quartet. This spectrum is inconsistent with the exclusive presence of the C_1-symmetric enantiomers **13** and **14** (eq 2) and reveals the presence of a small amount of the C_s-symmetric **15**, which shows identical chemical shifts (δ 5.01) for the enantiotopic H2,4 protons. Therefore, the two dominant H2,4 signals of equal area at δ 5.47 and 5.01 are assigned to **13** and **14**, in which the H2 and H4 protons are diastereotopic. The minor signal at δ 5.01 is assigned to **15**. Simulations of the H2,4 DNMR spectra at temperatures above 198 K required increasing concentrations of **15** (4% at 243 K, 6% at 262 K). The DNMR line-shape simulations also reveal that the rate of exchange between **13** and **14** (k_1 in eq 2 and Figure 5) is comparable to that for conversion of **13** (or **14**) to **15** (k_2 in eq 2 and Figure 5). The $\Delta G^{\ddagger}$ values for the **13** to **14** and **13** (or **14**) to **15** processes are 12.9 ± 0.3 and 12.4 ± 0.3 kcal mol^{-1}, respectively, at 252 K. The stereodynamics of **12** are different from those of the other complexes discussed above which do not show a detectable concentration of the C_s-symmetric conformation.

The H1,5 resonance shows a clear-cut decoalescence into two dominant signals at δ 4.47 and 1.44 (Figure 5, 198 K) that are due to conformations **13** and **14**. At 198 K, the resonance at δ 1.44 overlaps the H6 signal at δ 1.42 (Figure 5). We were not able to locate either by direct means or by inference from simulations a signal due to conformation **15**. In the calculation of the theoretical spectra in Figure 5, the H1,5 decoalescence was treated as a simple two-site exchange. The rate constants effective for acceptable simulations equal k_2 in Figure 5. In light of the presence of a small concentration of **15**, the H3, H6, and *exo*-phenyl ortho proton resonances will, in principle, decoalesce. While these signals show evidence of exchange broadening, signals due to the minor species could not be located.

The ^{1}H NMR subspectrum of the PCH_2CH_2P moiety at 303 K shows two differentially exchange-broadened signals at δ 3.53 and 3.02 overlapping the significantly broadened H1,5 resonance at δ 3.34 (Figure 5). Assignment of the methylene proton signals was confirmed by a separate examination of the complex having a perdeuterated cyclohexadienyl ring. At 303 K, cyclohexadienyl ring rotation is occurring at a rate that is moderately fast on the NMR chemical exchange time scale. The observation of two different methylene proton resonances at 303 K reveals that protons M and N in Figure 1 and in structure **16** (eq 3) maintain their integrity cis to the cyclohexadienyl ring

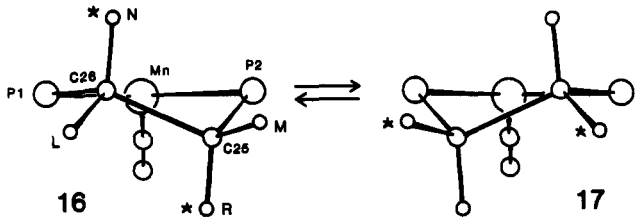

(3)

while protons L and R always remain trans to the cyclohexadienyl ring. This is consistent with an intramolecular conformational exchange process during which no ligand dissociation occurs. At temperatures below 303 K, the methylene proton subspectrum undergoes a complex decoalescence and, at 198 K, shows four dominant partially resolved multiplets at δ_L 3.92 (broad doublet), δ_M 3.67 (broad doublet), δ_N 3.53, and δ_R 2.14 (Figure 5). The observation of four signals shows that all four methylene protons are diastereotopic, consistent with the C_1 symmetry of **13** or **14** in eq 2. We were not able to locate the minor subspectrum of conformation **15**, most likely due to its low intensity and overlap with the dominant resonances. A salient feature of the spectrum is the two broad doublets at δ_L 3.92 and δ_M 3.67, each of which shows a large scalar coupling of ^{1}H to ^{31}P (38 Hz). While both $^2J_{HCP}$ and $^3J_{HCCP}$ values are dependent on stereochemistry, the absolute magnitude of $^3J_{HCCP}$ shows a greater dependence on stereochemistry than $^2J_{HCP}$.[20] The largest absolute value of $^3J_{HCCP}$ (+40 Hz) is about double that for $^2J_{HCP}$ (−20 Hz). $^3J_{HCCP}$ depends on dihedral angle in a manner analogous to the Karplus relationship for $^3J_{HCCH}$.[20] Therefore, the large proton–phosphorus coupling associated with the resonances at δ_L 3.92 and δ_M 3.67 is assigned logically to $^3J_{HCCP}$ and is typical for a H–C–C–P dihedral angle of about 180°. We assign the two doublets to the two equatorial protons L and M (see Figure 1 and structure **16** in eq 3), which are respectively anti to P2 and P1. While it is true that this scalar coupling could also be transmitted over the four-bond P–Mn–P–C–H framework, it is reasonable to presume that the three-bond coupling will dominate. The other two unresolved multiplets at δ_N 3.53 and δ_R 2.14 are due to the axial protons N and R in

(20) Quin, L. D. *The Heterocyclic Chemistry of Phosphorus*; Wiley-Interscience: New York, 1981; Chapter 6. Bentrude, W. G.; Setzer, W. N. In *Phosphorus-31 NMR Spectroscopy in Stereochemical Analysis. Organic Compounds and Metal Complexes*; Verkade, J. G.; Quin, L. D., Eds.; VCH: Deerfield Beach, FL, 1987; Chapter 11.

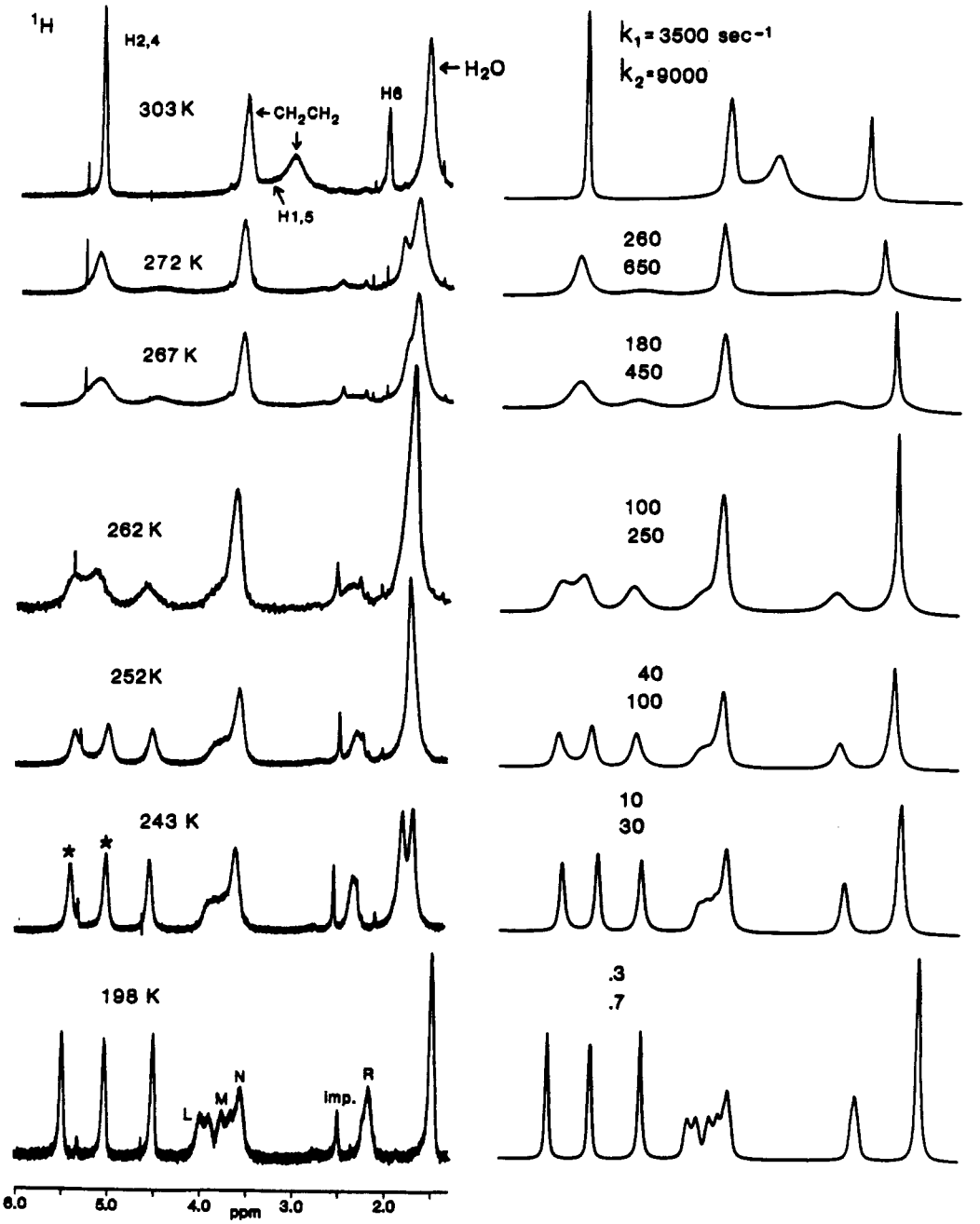

Figure 5. ^{1}H DNMR spectra (400.137 MHz) of the cyclohexadienyl H1,2,4,5,6 and PCH_2CH_2P protons of $[(PhC_6H_6)Mn(dppe)NO]PF_6$ (12) in $CDCl_3$. The rate constant k_1 is associated with interconversion between enantiomers 13 and 14 (eq 2; Y = NO); k_2 is associated with the 13 (or 14) to 15 process.

structure 16 that are associated with smaller dihedral angles (ca. 60°), with P2 and P1 leading to smaller $^3J_{HCCP}$ values (ca. 3 Hz) and more narrow multiplets. However, this analysis alone does not allow assignments of specific chemical shifts to individual protons on the metallacyclic ring.

As part of a rationale for assigning the methylene proton chemical shifts, it is noteworthy that the lowest frequency resonance at δ_R 2.14 reveals a proton that is subject to significantly greater diamagnetic shielding than the other three protons. Scrutiny of an accurate model of the molecular structure in the crystal shows that proton R (Figure 1 or structure 16 in eq 3) occupies a unique environment. Proton R is syn to the nitrosyl ligand and well within the shielding domains of *both* the C19 and C33 phenyl groups (Figure 1). Each of the other three methylene protons is located within the deshielding domain of the nearest phenyl group. On the basis of this observation, the signal at δ_R 2.14 is assigned to the axial proton R. While the methylene proton chemical shifts and the two large $^3J_{HCCP}$ values can be measured accurately, transverse relaxation broadening of the four complex multiplets at 198 K precluded the accurate measurement of other smaller coupling constants. However, by use of an iterative approach that employed a set of internally consistent coupling constants based on well-established trends for $^2J_{HCH}$, $^3J_{HCCH}$, $^2J_{HCP}$, and $^3J_{HCCP}$, we achieved an acceptable simulation of the methylene proton subspectrum at 198 K (Figure 5).[21] The NMR parameters used to achieve this simulation are listed in Table VII. No attempt was made to include a minor subspectrum due to conformation 15. The simulation incorporates a coupling constant of −14 Hz between the two protons giving signals at δ_M 3.68 and δ_R 2.14. This is

(21) Johannesen, R. B.; Ferretti, J. A.; Harris, R. K. Quantum Chemistry Program Exchange (Indiana University), 1985, No. 188.

Table VII. NMR Parameters for the ^1H PCH_2CH_2P Subspectrum of the C_1-Symmetric Enantiomeric Conformations of $[(PhC_6H_6)Mn(NO)dppe]PF_6$

^1H chem shift, ppm[a]	δ_L 3.92, δ_M 3.67, δ_N 3.53, δ_R 2.14
coupling constant, Hz	$^3J_{LM} = 4$, $^2J_{LN} = -13$, $^3J_{LR} = 6$, $^2J_{LP1} = -11$, $^3J_{LP2} = 38$, $^3J_{MN} = 4$, $^2J_{MR} = -14$, $^3J_{MP1} = 38$, $^2J_{MP2} = -11$, $^3J_{NR} = 6$, $^2J_{NP1} = -17$, $^3J_{NP2} = 2$, $^3J_{RP2} = -17$, $^3J_{P1P2} = 13$

[a] See Figure 1 and structure **16** in eq 3 for assignments. In the $^{31}P\{^1H\}$ spectrum at 198 K, the two ^{31}P chemical shifts for enantiomers **13** and **14** are separated by 1.30 ppm.

a typical $^2J_{HCH}$ value for an sp^3-hybridized methylene carbon and suggests that protons M and R are on the same carbon atom. The resonance at δ_M 3.68 is assigned to the equatorial proton M in Figure 1 and in **16**. The equatorial proton L (Figure 1 and **16**) that is anti to P2 is then logically assigned to the other broad doublet at δ_L 3.92, which shows a large $^3J_{HCCP}$ value. Finally, the resonance at δ_N 3.53 is assigned to the axial proton N.

During the course of the conversion of **13** to its enantiomer **14** (eq 2), the chiral metallacyclic moiety **16** (eq 3) is converted to its enantiomer **17**. During this process, equatorial proton L and axial proton R mutually exchange molecular environments while axial proton N and equatorial proton M interchange sites. Consistent with the chemical shift assignments above and the metallacyclic enantiomerization shown in eq 3, and the dominance of conformations **13** and **14**, adequate simulations of the DNMR spectra of the methylene protons were achieved by using a LMNRXY to RNMLYX (X = Y = ^{31}P) magnetization exchange itinerary. The effective rate constants equal k_2 in Figure 5. While the simulations of the methylene proton DNMR spectra do not include the minor subspectrum due to **15** and must be considered approximate, it is reasonable to conclude that the rates of cyclohexadienyl ring rotation and metallacyclic ring stereomutation are equal and that these two processes do occur in concert. In light of the generally very low barriers to stereomutation in five-membered rings, it is probable that cyclohexadienyl ring rotation drives metallacyclic ring stereomutation. The metallacyclic ring adjusts its geometry in response to the orientation of the cyclohexadienyl ring.

The $^{31}P\{^1H\}$ NMR spectrum (161.978 MHz) of **12** in CD_2Cl_2 at 295 K shows an exchange-broadened singlet at δ 74.17. At lower temperatures, the spectrum decoalesces asymmetrically into two resonances. In the decoalesced but still exchange-broadened spectrum at 236 K, the lower frequency signal has a perceptively greater peak area than the higher frequency signal. At 199 K, the spectrum is sharpened ostensibly into an AX spectrum. However, the spectrum is asymmetric. The lower frequency component of the lower frequency doublet has a perceptively higher intensity than the higher frequency component of the higher frequency doublet. The 199 K spectrum is stimulated accurately as a dominant AX spectrum (98%; δ_A 70.78, δ_X 69.48; J_{PP} = 13 Hz) superimposed on a minor singlet resonance at δ_Y 69.42 (2%). The AX spectrum is assigned to enantiomers **13** and **14** in eq 2 (Y = NO), in which the phosphorus atoms are diastereotopic. The lower frequency resonance at δ_X 69.48 is assigned to the phosphorus atom that eclipses C4 in **13** or C2 in **14** and is located in the shielding domain of the cyclohexadienyl ring.[8] The signal at δ_A 70.78 is assigned to the phosphorus atom that eclipses C6 in **13** or **14** and is removed from the shielding effects of the cyclohexadienyl π-system. The minor singlet at δ_Y 69.42 is assigned logically to the C_s-symmetric conformation **15**, in which the phosphorus atoms are enantiotopic, will show identical chemical shifts, and are both subject to the shielding effects of the cyclohexadienyl ring. In the simulation of the DNMR spectra, the AX to XA exchange of magnetization corresponds to exchange between enantiomers **13** and **14** (k_1 in eq 2) and the AX (or XA) to Y_2 transfer corresponds to conversion of **13** (or **14**) to **15** (k_2 in eq 2). In a manner analogous to the DNMR behavior of the H2,4 resonances, simulation of the $^{31}P\{^1H\}$ DNMR spectra at increasing temperatures required increasing amounts of the minor species **15**. The $\Delta G^\ddagger$ values at 242 K for the k_1 process (12.6 ± 0.3 kcal/mol) and the k_2 process (12.2 ± 0.3 kcal/mol) agree with those obtained from simulations of the ^1H DNMR spectra of the cyclohexadienyl H2,4 protons (vide supra). ^{31}P NMR parameters for **12** and other complexes are listed in Table VIII.

Both the ^1H and $^{31}P\{^1H\}$ DNMR spectra of **12** reveal a strong conformational preference for the enantiomeric conformations **13** and **14** with a small but detectable concentration of the achiral species **15**. The barrier to exchange between **13** and **14** is comparable to but slightly greater than conversion of either enantiomer to the achiral conformation **15**. As shown in Table V, the rotation barriers in **12** are about 1 and 2 kcal mol^{-1} higher, respectively, than those in $[(PhC_6H_6)Mn(NO)(PMe_3)_2]PF_6$ and $[(PhC_6H_6)Mn(CO)_2NO]PF_6$. These barrier differentials may be due to electronic effects of the different ligands and/or increased steric crowding in **12**. Some of the barrier differentials could also arise from vicinal proton–proton eclipsing in the CH_2CH_2 moiety of **12** as the metallacyclic ring inverts (eq 3) in concert with cyclohexadienyl ring rotation.

The crystal and molecular structure of **$(PhC_6H_6)Mn(dppe)CO$ (18)** and its corresponding radical cation (18^+) have been determined by X-ray crystallography.[14] In the solid state, **18** and 18^+ both adopt the C_s-symmetric conformation **15** (eq 2; Y = CO). The $^{31}P\{^1H\}$ NMR spectrum of **18** in CD_2Cl_2 at 300 K shows a singlet at δ 107.5 (Figure 6) consistent with rapid conformational exchange. At lower temperatures, the spectrum decoalesces asymmetrically and, at 183 K, is sharpened into two singlets of equal area (δ 117.5 (32.5%), δ 113.1 (32.5%)) and a third singlet at δ 103.5 (35.0%). The two singlets of equal area at δ 117.5 and 113.1 are assigned logically to the C_1-symmetric enantiomers **13** and **14** in eq 2 (Y = CO) in which the phosphorus atoms are diastereotopic. The phosphorus atom that eclipses C4 in **13** or C2 in **14** and is in the

Table VIII. ^{31}P NMR Data for (Cyclohexadienyl)manganese Complexes with Bidentate Ligands

complex	temp, K	chem shift, ppm
$[(PhC_6H_6)Mn(NO)dppe]PF_6$ **(12)**[a]	295	74.2 (br s)
	205	AX spectrum (98%; 70.8, 69.5, J_{PP} = 13 Hz); singlet (2%; 69.4)
$(PhC_6H_6)Mn(CO)dppe$ **(18)**[b]	300	107.5 (br s)
	183	117.5 (s, 32.5%), 113.1 (s, 32.5%), 103.5 (s, 35%)
$[(PhC_6H_6)Mn(NO)arphos]PF_6$ **(19)**[b]	301	93.3 (br s)
	231	99.1 (s, 88%), 92.6 (s, 12%)

[a] In $CDCl_3$: broad-band decoupled, referenced to external H_3PO_4 (0 ppm). [b] In CD_2Cl_2.

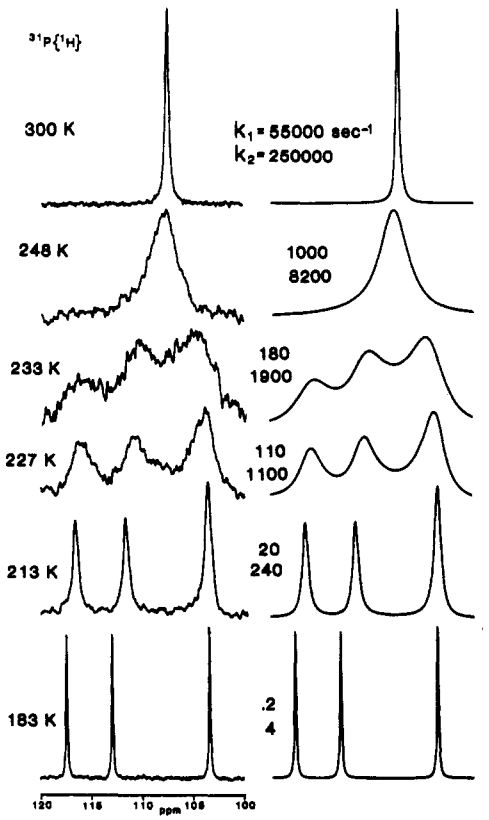

Figure 6. $^{31}P\{^1H\}$ DNMR spectra (161.958 MHz) of (PhC_6H_6)-Mn(dppe)CO (18) in CD_2Cl_2. The rate constant k_1 is associated with interconversion between enantiomers 13 and 14 (eq 2; Y = CO); k_2 is associated with the 13 (or 14) to 15 process.

shielding domain of the cyclohexadienyl ring is assigned the chemical shift at δ 113.1.[8] The unique singlet at δ 103.5 is assigned to 15, in which the enantiotopic phosphorus atoms will have identical chemical shifts and are located in the shielding region of the cyclohexadienyl ring. The 183 K spectrum reveals conformational preferences for 18 dramatically different from those for all the other complexes discussed above. At 183 K, there is 65% of the enantiomers 13 and 14 and 35% of the C_s-symmetric 15. The distribution of conformational populations is essentially statistical, suggesting small enthalpy and entropy differences between 13 (or 14) and 15. In contrast, the difference in free energy between the preferred 13 (or 14) and 15 in complex 12 (eq 2; Y = NO) is about 1.3 kcal mol^{-1} at 198 K. For the other complexes discussed above, the C_s-symmetric conformation is so unstable as to be undetectable. For 18, the presence of significant concentrations of all three conformers in eq 2 allows accurate determinations of the rates of different exchange itineraries (k_1, k_2) by simulation of the DNMR spectra (Figure 6). The simulations reveal that there is a higher barrier for direct exchange between 13 and 14 ($\Delta G^\ddagger$ = 11.1 ± 0.1 kcal mol^{-1} at 227 K) than for conversion of 13 (or 14) to 15 ($\Delta G^\ddagger$ = 10.0 ± 0.1 kcal mol^{-1} at 227 K). The kinetics are analogous to those for complex 12 (eq 2; Y = NO; vide supra).

The ^1H DNMR spectra of 18 allow a corroboration of the stereodynamics gleaned from the $^{31}P\{^1H\}$ DNMR behavior. For example, the H2,4 protons show a single multiplet (δ 4.42) at 298 K that decoalesces asymmetrically at lower temperatures. At 183 K, the H2,4 subspectrum is sharpened into two resonances of equal area at δ 4.72 (33%) and δ 4.33 (33%) that are assigned to conformers 13 and 14 (eq 2) and a third signal at δ 4.35 (34%) that is assigned to 15. The barriers determined from simulations of the ^1H DNMR spectra for the k_1 process (eq 2; $\Delta G^\ddagger$ = 11.2 ± 0.2 kcal mol^{-1} at 213 K) and for the k_2 process ($\Delta G^\ddagger$ = 10.2 ± 0.2 kcal mol^{-1} at 213 K) agree very well with those determined from the $^{31}P\{^1H\}$ DNMR spectra. Thus, both sets of spectra corroborate an essentially statistical distribution of equilibrium conformations and a higher barrier for the k_1 conversion in eq 2.

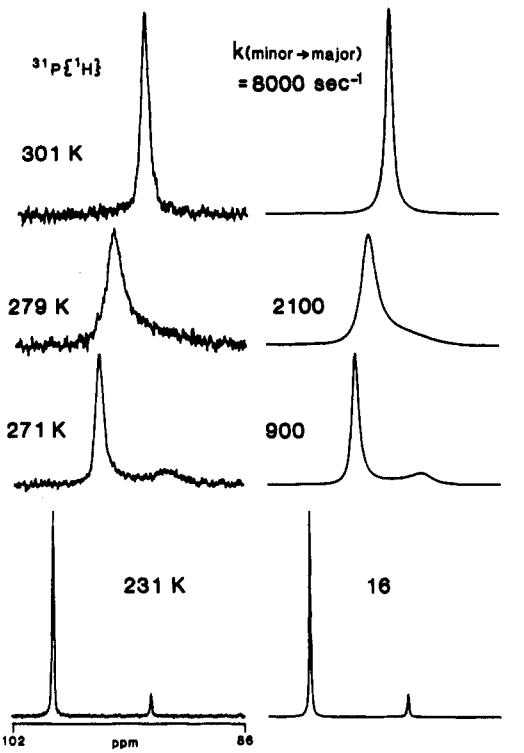

Figure 7. $^{31}P\{^1H\}$ DNMR spectra (161.958 MHz) of $[(PhC_6H_6)Mn(arphos)NO]PF_6$ (19) in CD_2Cl_2. The rate constant k is associated with the conversion of conformation 21 to 20 (see text).

The arphos complex **$[(PhC_6H_6)Mn(arphos)NO]PF_6$** (19) possesses a chiral center at manganese. Unfortunately, attempts to determine the crystal and molecular structure of 19 by using X-ray crystallography were unsuccessful due to disorder in the crystal. Complex 19 exists as a pair of enantiomers. For one enantiomer, all three of the cyclohexadienyl ring rotamers (20–22) are diastereomeric and,

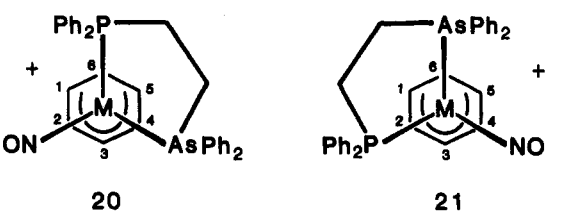

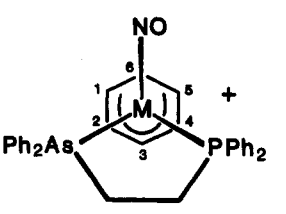

in principle, will have different stabilities and different spectroscopic properties. The $^{31}P\{^1H\}$ NMR spectrum of 19 in CD_2Cl_2 at 301 K shows an exchange-broadened singlet at δ 93.30 that decoalesces into two singlets of significantly different areas (Figure 7). At 231 K, the spectrum consists of one singlet at δ 99.12 (88%) and another at δ 92.61 (12%), revealing the presence of two

diastereomeric conformations having different concentrations. The free energy preference for the major conformation is 0.9 kcal mol^{-1} at 231 K. Simulations of the DNMR spectra at increasing temperatures required the use of increasing amounts of the minor species (i.e., 12% at 231 K, 17% at 256 K, 23% at 271 K). The $\Delta G^{\ddagger}$ value for conversion of the minor to the major species is 12.1 ± 0.1 kcal mol^{-1} at 279 K.

The ^{1}H NMR spectrum of **19** in CD_2Cl_2 at 308 K shows a series of differentially exchange-broadened resonances punctuated by sharp signals due to H3 (t, δ 6.70), the ortho protons on the 6-*exo*-phenyl group (dd, δ 6.52), H2 or H4 (δ 5.29; overlaps the solvent signal), H2 or H4 (q, δ 5.17), and H6 (t, δ 2.28). Resonances that are almost exchange-broadened into the base line are centered at δ 4.22 (H1 or H5) and at δ 2.75 (H1 or H5). The observation of six different cyclohexadienyl ring proton signals under conditions of moderately fast cyclohexadienyl ring rotation attests to the chirality of **19** and that, even under conditions of rapid conformational exchange among rotamers **20–22**, the H2,4 (and H1,5) protons are not allowed a mutual exchange of molecular environments. Consequently, the time-averaged environments and chemical shifts of all six diastereotopic ring protons will be different. In addition to the cyclohexadienyl ring proton signals, the PCH_2CH_2As moiety shows two well-resolved multiplets at δ 3.53 and 3.31 in addition to two unresolved, exchange-broadened signals at δ 3.42 and 2.52. The observation of four methylene proton resonances is consistent with the chirality of **19** and the fact that none of the methylene protons are allowed a mutual exchange of molecular environments as a result of intramolecular cyclohexadienyl ring rotation.

At lower temperatures, the ^{1}H NMR spectrum shows a complex decoalescence and, at 228 K, is sharpened into a slow-exchange spectrum. A portion of that spectrum is shown at the bottom of Figure 8. Consistent with the $^{31}P\{^1H\}$ NMR spectrum at 231 K (Figure 7), the ^{1}H spectrum at 228 K is simulated accurately by superimposing a dominant subspectrum (90%) upon a minor subspectrum (10%) as shown in Figure 8. The dominant subspectrum shown at the top of Figure 8 includes six cyclohexadienyl ring proton signals at δ 6.88 (t, H3), 5.53 (t, H2 or H4), 5.12 (q, H2 or H4), 4.85 (t, H1 or H5), 1.89 (H6), and 1.60 (q, H1 or H5), and a doublet at δ 6.38 due to the ortho protons on the 6-*exo*-phenyl group. The dominant PCH_2CH_2As subspectrum shows a septet at δ_X 2.02 due to a proton that is significantly shielded, a triplet of doublets at δ_F 3.31, a triplet of doublets at δ_B 3.76, and a doublet of "quartets" at δ_A 3.85 that reveals a large proton–phosphorus coupling equal to 38 Hz. The lower frequency quartet of the A resonance overlaps the B signal. The A resonance is assigned to a proton that is equatorial on the metallacyclic ring and anti to the phosphorus (vide supra).[20] The NMR parameters used to simulate the major PCH_2CH_2As subspectrum are listed in Table IX. The minor subspectrum (Figure 8) consists of six cyclohexadienyl ring proton resonances at δ 6.73 (H3), 5.53 (H2 or H4), 5.00 (H2 or H4), 4.58 (H1 or H5), 1.77 (H1 or H5), and 1.77 (H6) as well as an *exo*-phenyl ortho proton resonance at δ 6.48. The PCH_2CH_2As moiety shows two unresolved signals centered at δ 3.43 (3 H) and 2.66 (1 H). In light of the fact that the PCH_2CH_2As resonances show no fine structure due to T_2 relaxation and possibly a small rate of conformational exchange, any simulation must be considered tentative. However, a reasonable fit of the subspectral envelope was achieved by using the NMR parameters listed in Table IX. It is noteworthy that the signal at δ_D 3.42 apparently shows

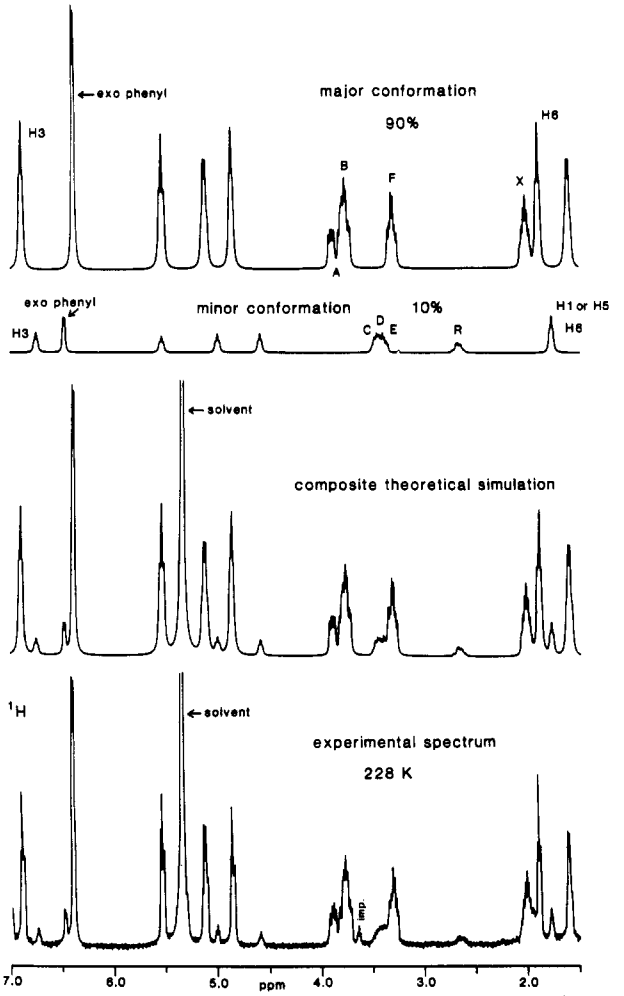

Figure 8. Decomposition of the theoretical simulation of the slow-exchange ^{1}H NMR spectrum (400.137 MHz) of the cyclohexadienyl ring, PCH_2CH_2As, and 6-*exo*-phenyl ortho protons of $[(PhC_6H_6)Mn(arphos)NO]PF_6$ (**19**) in CD_2Cl_2 at 228 K. Subspectra due to the major (**20**, see text) and minor (**21**) conformations are shown at the top of the figure. Superposition of the two subspectra and addition of the solvent resonance ($CHDCl_2$) produce the composite theoretical simulation. The experimental spectrum is shown at the bottom of the figure.

Table IX. NMR Parameters Used To Simulate the PCH_2CH_2As Portion of the ^{1}H NMR Spectrum of $[(PhC_6H_6)Mn(NO)arphos]PF_6$ (19) at 228 K

Major Conformation (90%)[a]	
^{1}H chem shift, ppm	δ_A 3.85, δ_B 3.76, δ_F 3.31, δ_X 2.02
coupling constant, Hz	J_{AB} = 1, J_{AF} = 7, J_{AX} = −14, J_{AP} = 38,[b] J_{BF} = −14, J_{BX} = 6, J_{BP} = 14,[b] J_{FX} = 14, J_{FP} = 0,[b] J_{XP} = 7[b]
Minor Conformation (10%)[a]	
^{1}H chem shift, ppm	δ_C 3.46, δ_D 3.42, δ_E 3.40, δ_R 2.66
coupling constant, Hz	J_{CD} = 7, J_{CE} = −14, J_{CR} = 14, J_{CP} = 5,[b] J_{DE} = 1, J_{DR} = −14, J_{DP} = 38,[b] J_{ER} = 6, J_{EP} = 14,[b] J_{RP} = 12[b]

[a] Some tentative assignments are in the text. [b] P = ^{31}P.

a large proton–phosphorus coupling due to a proton that is equatorial on the metallacyclic ring and anti to phosphorus.[20] Superposition of the major subspectrum (90%) on the minor subspectrum (10%) and addition of the solvent signal produces the composite theoretical simulation in Figure 8 that shows an acceptable fit to the experimental spectrum at the bottom of Figure 8.

In both of the subspectra in Figure 8, and H1 and H5 signals are widely spaced. This is reminiscent of the

slow-exchange spectrum of the dppe analogue (Figure 5) that shows a strong preference for enantiomers **13** and **14** (eq 2; Y = NO). In **13** or **14**, H1 and H5 are located in significantly different molecular environments and are subject to significantly different diamagnetic shielding. The environments of H1 and H5 in **20** and **21** are highly analogous to those in **13** or **14**. While **22** is chiral, it does possess a pseudo plane of symmetry; H1 and H5 are located in similar molecular environments and would not be expected to have the widely divergent chemical shifts shown in either subspectrum in Figure 8. Similar arguments can be made for H2 and H4. Therefore, the two subspectra in Figure 8 are consistent with conformations **20** and **21** and not with **22**. However, the ^{1}H spectra do not allow assignment of either subspectrum to a specific conformation. In this regard, the ^{31}P{^{1}H} NMR spectrum at 231 K (Figure 7) is informative. The minor singlet at δ 92.61 reveals a phosphorus atom that is shielded relative to the one that gives the resonance at δ 99.12. The resonance at δ 92.61 is assigned logically to the phosphorus atom in **21** that is in the shielding region of the cyclohexadienyl π-system.[8] Therefore, the minor conformer of **19** is assigned to **21**. The major conformation is assigned to **20**, in which the phosphorus atom is removed from the shielding region of the π-system. A reasonable three-dimensional representation of **20** might be Figure 1 if P2 is replaced by As. The metallacyclic ring might be represented by **16** if P2 is replaced by As. Consistent with these conformational assignments, the shielded methylene proton resonance at δ_X 2.02 in the major subspectrum of **19** at 228 K (Figure 8) is assigned to proton R in Figure 1 (P2 = As). In the major subspectrum, the doublet of quartets at δ_A 3.85 that shows a strong coupling of ^{1}H to ^{31}P is assigned to proton M that is anti to phosphorus (vide supra).[20] Assignments of the other two methylene proton signals are problematical.

Acceptable simulations of the ^{1}H DNMR spectra of **19** were achieved by using seven separate two-site exchanges of magnetization of the cyclohexadienyl ring and 6-*exo*-phenyl ortho protons. The ^{1}H DNMR behavior of the methylene proton subspectrum is simulated adequately by using an ABFXP to RECDP* (P = P* = ^{31}P) exchange of magnetization (Figure 8). It is satisfying that resonance A (major species; large $^3J_{HCCP}$) exchanges with signal R (minor species; small $^3J_{HCCP}$), consistent with an equatorial to axial exchange of sites on the metallacyclic moiety. From a complete simulation of the exchange-broadened spectrum at 273 K, the rate constants for transfer of magnetization from the various signals of the minor conformation to their respective exchange partners in the major conformation, including the methylene proton subspectrum, are all equal at 1200 s^{-1}. This gives a ΔG^* value (12.1 ± 0.3 kcal mol^{-1}) which is identical with that derived from the ^{31}P{^{1}H} DNMR spectra. Thus, in a manner strictly analogous to the dppe and dppen analogues, stereomutation of the metallacyclic ring occurs in concert with cyclohexadienyl ring rotation. It is also clear that, in this chiral complex, the various diastereomeric conformations are present in significantly different concentrations.

As stated above, disorder precluded obtaining the crystal and molecular structure of **19** by using X-ray crystallography. It remains interesting to determine the conformational makeup of **19** in the crystalline state. At progressively lower temperatures, the half-life of **20** or **21** gets progressively longer and longer. At a sufficiently low temperature that can be predicted from the activation parameters derived from simulations of the DNMR spectra, the half-lives will become long enough to allow isolation of **20** or **21** on the laboratory time scale. A sample of a solvent mixture consisting of 20% CD_2Cl_2/70% $CHCl_2F$/10% $CHClF_2$ was placed in an NMR tube in a vacuum-jacketed cooling chamber equipped with a viewing window and cooled to 150 K. A crystalline sample of **19** was dropped into the solvent and the mixture stirred for 1 h until all the crystals had dissolved. The sample was transferred quickly to an NMR probe at 150 K and the ^{31}P{^{1}H} NMR spectrum recorded. The spectrum showed one singlet at δ 103.7 and no other detectable signals. The 150 K spectrum reveals the solution of a conformationally pure form of **19** that is prevented from equilibration to any other conformations by the long half-life at 150 K. The spectrum shows that the crystalline state of **19** is conformationally homogeneous. The chemical shift of the lone singlet correlates well with the major singlet in the 231 K spectrum of **19** in Figure 7 and, on the basis of our conformational assignments above, is assigned to **20** and its enantiomer. Over a 2.5-h period at 150 K, there was no evidence of the appearance of any other resonances that would appear as a result of a conformational equilibration. At 180 K, a minor singlet at δ 95.0 appeared and grew in intensity with time, indicating equilibration of **20** to **21**. While it was not possible to solve the crystal structure of **19**, this experiment does show that the crystals are conformationally homogeneous as **20** and its enantiomer.

Summary

For a series of 6-*exo*-phenylcyclohexadienyl and 6-*exo*-phenyl-1,2,3,4,5-pentamethylcyclohexadienyl complexes of manganese and rhenium, the ^{1}H and/or ^{31}P{^{1}H} NMR spectra show decoalescence below room temperature due to restricted cyclohexadienyl ring rotation. Theoretical simulations of a slow-exchange spectrum and the exchange-broadened DNMR spectra for each complex allowed identification of the preferred equilibrium conformations and calculation of the barrier(s) to conformational exchange. For the series of complexes in Table V that have three unidentate ligands, two of the unidentate ligands are identical and one is unique. For each of these complexes, there is an exclusive preference for the C_1-symmetric enantiomers **5** and **6** (eq 1), in which the unique unidentate ligand eclipses C4 or C2 of the cyclohexadienyl ring. It is apparent that the nitrosyl ligand prefers essentially exclusively to eclipse C2 or C4 of the cyclohexadienyl ring. The barriers (ΔG^*) to enantiomerization fall in the range of 9.2–11.4 kcal mol^{-1}. For all these systems, the ΔS^* values for conformational exchange are small, indicating that the barriers are predominantly enthalpic in origin. The small ΔS^* values also argue against a mechanism for conformational exchange that involves any ligand dissociation. Replacement of a CO ligand by NO^+ or PMe_3 increases the barrier, while substitution of rhenium for manganese has no effect (Table V).

For a series of four 6-*exo*-phenylcyclohexadienyl complexes of manganese that possess a bidentate ligand, the conformational preferences vary significantly (Table V). For the dppen/NO system, there is an exclusive preference for the C_1-symmetric enantiomers (e.g. **10**). In the dppe/NO derivative, the C_1 conformers (**13** and **14**, eq 2, Y = NO) are dominant (98%) but about 2% of the C_s conformation **15** is present at 199 K. The barrier for interconversion of the C_1 conformers (ΔG^* = 12.9 kcal mol^{-1}) is slightly higher than that for conversion of the C_1 species to the C_s form (ΔG^* = 12.4 kcal mol^{-1}). Theoretical simulations of the ^{1}H DNMR spectra of the cyclohexadienyl ring protons and the dppe methylene protons show that cyclohexadienyl ring rotation occurs in concert with me-

tallacyclic ring stereomutation. For the dppe/CO complex, there is an essentially statistical distribution of populations among the enantiomeric C_1 conformers and the C_s species (eq 2; Y = CO). The barrier for interconversion between the C_1 conformers (11.1 kcal mol^{-1}) is higher than that for conversion of a C_1 form to the C_s species (10.0 kcal mol^{-1}). The chiral arphos/NO complex shows a strong preference for conformer **20** (88% at 231 K), in which phosphorus eclipses C6 of the cyclohexadienyl ring, and a smaller amount of **21** (12%), in which arsenic eclipses C6. In both detectable conformations, NO eclipses a carbon in the π-system of the cyclohexadienyl ring. The barrier for conversion of **21** to **20** is 12.1 kcal mol^{-1}.

Acknowledgment. Valuable and expert assistance by Dr. J. Van Epp (NMR) and Professor G. B. Carpenter (X-ray) is gratefully acknowledged. This work was supported by grants from the National Science Foundation to D.A.S. (Nos. CHE-8521189 and CHE-8821588). C.H.B. is grateful to the University of Vermont (UVM) Academic Computing Center for computational support and to the UVM University Committee on Research and Scholarship for partial financial support.

Registry No. 4, 81971-52-0; 8, 122648-18-4; 9, 127518-84-7; 12, 127518-82-5; 18, 98150-66-4; 18$^+$, 98150-67-5; [(PhC_6H_6)Mn(NO)arphos]PF_6, 142042-19-1; (PhC_6H_6)$Mn(CO)_2PMe_3$, 125333-95-1; [(PhC_6H_6)$Mn(NO)(PMe_3)_2$]PF_6, 142042-17-9; [(PhC_6HMe_5)$Mn(CO)_2NO$]PF_6, 122648-24-2; (PhC_6H_6)Mn(CO)$(PMe_3)_2$, 125432-83-9; (6-*exo*-Ph-5-*exo*-PMe_3-η^4-C_6H_6)Mn(CO)(NO)PMe_3^+, 142065-28-9.

Supplementary Material Available: Tables of hydrogen coordinates and anisotropic thermal parameters for [(PhC_6H_6)Mn(NO)dppe]PF_6 (12) (2 pages). Ordering information is given on any current masthead page.

OM9107348

Binuclear Cyclopentadienyl Carbonyl Complexes of Molybdenum(I) with Bidentate Phosphorus Bridging Ligands: Synthesis and Reactions Leading to New Dimolybdenum(II) Complexes

Víctor Riera* and Miguel A. Ruiz

Departamento de Química Organometálica, Universidad de Oviedo, 33071 Oviedo, Spain

Fernando Villafañe

Departamento de Química Inorgánica, Universidad de Valladolid, 47005 Valladolid, Spain

Received December 26, 1991

The compounds (μ-P-P)$Mo_2Cp_2(CO)_4$ (Cp = η^5-C_5H_5; P-P = $Ph_2PCH_2PPh_2$, dppm; $(EtO)_2POP(OEt)_2$, tedip) were prepared from $Mo_2Cp_2(CO)_4$ (Mo≡Mo) and dppm or tedip, respectively. In the reaction with tedip, the compound (μ-$(EtO)_2PO$)(μ-$P(OEt)_2$)$Mo_2Cp_2(CO)_4$ was also isolated. The dppm-bridged compound reacted with different electrophiles to give new dimolybdenum(II) complexes. Thus, reaction with HBF_4 or $[Ipy_2]BF_4$ (py = pyridine) gave the compounds [(μ-X)(μ-dppm)$Mo_2Cp_2(CO)_4$]BF_4 (X = H, I), whereas reaction with the electrophiles I_2 or $HgCl_2$ gave (X)$(CO)_2$CpMo(μ-dppm)MoCp$(CO)_2$(Y) (X = Y = I; X = ClHg, Y = Cl). The related (μ-dppm)$Mo_2Cp_2(CO)_4Cl_2$ could be obtained by treatment of $MoCp(CO)_3Cl$ with dppm. The reduction of (μ-dppm)$Mo_2Cp_2(CO)_4$ with sodium amalgam led to the anion Na_2[(μ-dppm)$Mo_2Cp_2(CO)_4$], which was used in situ to obtain new dimolybdenum(II) species. Protonation of the anion with NH_4PF_6 gave the dihydrido complex (μ-dppm)$Mo_2Cp_2(CO)_4H_2$, and treatment with CH_2I_2 or $(ClCuPPh_3)_4$/Ph_4AsCl led to (ICH_2)$(CO)_2$CpMo(μ-dppm)MoCp$(CO)_2$I or to the trinuclear anion Ph_4As[(μ-$CuPPh_3$)(μ-dppm)$Mo_2Cp_2(CO)_4$], respectively. The presence of different isomers in some of the compounds described and the influence of the solvent and temperature on the corresponding equilibria are discussed.

Introduction

The chemical behavior of the metal–metal bonds present in organometallic complexes is currently the object of intensive studies. Although the interest in this type of complexes is widespread, their catalytic activity is deserving of most attention. An analogy may be established between the chemical activity of the metal–metal bonds and the ability of some metallic surfaces to adsorb small molecules, and therefore bimetallic systems can be considered the simplest link between homogeneous and heterogenous catalysts.[1] Their potential superconductivity or biomedical uses are other applications already reported.[2] However, the study of the reactivity of complexes containing metal–metal bonds is frequently limited by the tendency of the system to give mononuclear compounds.[3] Dimer degradation is generally avoided by the use of bridging ligands, which maintain the nuclearity of the complex. In particular, bidentate phosphorus-donor ligands of the type A_2PBPA_2 (A = R, OR; B = CH_2, NR', O; R = alkyl, aryl) have proved to be useful in this role.[4]

(1) (a) Chini, P. *J. Organomet. Chem.* **1980**, *29*, 1. (b) Muetterties, E. L.; Stein, J. *Chem. Rev.* **1979**, *79*, 479. (c) Vahremkamp, H. *Angew. Chem., Int. Ed. Engl.* **1978**, *17*, 379.

(2) (a) Mingos, D. M. P. *Acc. Chem. Res.* **1984**, *17*, 311. (b) Jaouen, G.; Vessières, A.; Top, S.; Savignac, M.; Ismail, A. A.; Butler, I. S.; *Organometallics* **1987**, *6*, 1985.

(3) Chisholm, M. H.; Rothwell, I. P. *Prog. Inorg. Chem.* **1982**, *29*, 1.

(4) (a) Puddephatt, R. J. *Chem. Soc. Rev.* **1983**, *12*, 99. (b) Chaudret, B.; Delavaux, B.; Poilblanc, R. *Coord. Chem. Rev.* **1988**, *86*, 191. (c) King, R. B. *Acc. Chem. Res.* **1980**, *13*, 243. (d) Riera, V.; Ruiz, M. A. *J. Chem. Soc., Dalton Trans.* **1986**, 2617.

0276-7333/92/2311-2854$03.00/0